

# Empirical Analysis of Nature-Inspired Algorithms for Autism Spectrum Disorder Detection Using 3D Video Dataset

Aneesh Panchal<sup>1,3</sup>, Kainat Khan<sup>2,3</sup>, and Rahul Katarya<sup>3,\*</sup>

<sup>1</sup>Department of Computational and Data Sciences, Indian Institute of Science, Bangalore, Karnataka–560012, INDIA

<sup>2</sup>Indian Institute of Information Technology, Dharwad, Karnataka–580009, INDIA

<sup>3</sup>Big Data Analytics and Web Intelligence Laboratory, Department of Computer Science & Engineering, Delhi Technological University, New Delhi–110042, INDIA

<sup>1</sup>Email: aneeshpanchal840850@gmail.com

<sup>2</sup>Email: khankainat388@gmail.com

\*Corresponding author: rahuldtu@gmail.com

## Abstract

Autism Spectrum Disorder (ASD) is a chronic neurodevelopmental condition characterized by repetitive behaviors and impairments in social and communication skills. Despite the clear manifestation of these symptoms, many individuals with ASD remain undiagnosed. This paper proposes a methodology for ASD detection using a three-dimensional walking video dataset, leveraging supervised machine learning classification algorithms combined with nature-inspired optimization algorithms for feature extraction. The approach employs supervised classifiers to identify ASD cases, while nature-inspired optimization techniques select the most relevant features, enhanced by the use of ranking coefficients to identify initial leading particles. This strategy significantly reduces computational time, thereby improving efficiency and accuracy. Experimental evaluation with various algorithmic combinations demonstrates an exceptional classification accuracy of 100% in the best case when using the Random Forest classifier coupled with the Gravitational Search Algorithm for feature selection. The methodology's application to additional datasets promises improved robustness and generalizability. With its high accuracy and reduced computational requirements, the proposed framework offers significant contributions to both medical and academic fields, providing a foundation for future advances in ASD diagnosis.

**Keywords** - Autism spectrum disorder; Machine learning; Nature-inspired algorithm; Ranking coefficient; 3D walking human video dataset.

## 1 Introduction

Autism Spectrum Disorder (ASD) is a chronic neurodevelopmental condition characterized by challenges in social communication, restricted interests, and repetitive behaviors. Early diagnosis of ASD is critical, as timely intervention can significantly improve social, emotional, and cognitive outcomes. Conventional diagnostic tools such as the Autism Diagnostic Observation Schedule (ADOS), Childhood Autism Rating Scale (CARS), and Autism Diagnostic Interview-Revised (ADI-R) are widely used in clinical practice. While these instruments are considered reliable, they rely heavily on subjective expert assessment, are time-consuming, and often require specialized clinical training. This has led to delayed or missed diagnoses, particularly in resource-constrained settings.

To address these limitations, researchers have increasingly turned to computational and data-driven approaches that leverage behavioral, physiological, and multimodal data for ASD detection. In particular, gait and movement patterns are gaining attention as potential digital biomarkers, since motor abnormalities such as atypical stride length, postural instability, or irregular hand-knee coordination are frequently observed in children with ASD. Compared to invasive or clinical assessment procedures, gait-based video analysis is non-intrusive, cost-effective, and scalable, making it well-suited for real-world deployment.

## 1.1 Motivation

The prevalence of ASD continues to increase worldwide. Recent estimates suggest that approximately 1 in 68 children in the United States and 1 in 500 children in India are diagnosed with ASD, with rising numbers also being reported across Europe, including France. According to the World Health Organization (WHO), nearly 1–1.5% of the global population may fall on the autism spectrum. In India, underdiagnosis remains a critical challenge due to limited clinical infrastructure, whereas in France, recent reports have emphasized the necessity of improved early screening practices within schools and healthcare centers. These circumstances collectively underscore the urgent need for automated, scalable, and interpretable diagnostic support systems.

Machine Learning (ML) techniques have demonstrated significant potential in detecting ASD across diverse modalities, including eye-gaze patterns, physiological signals, speech, and facial movement data. However, the use of high-dimensional gait video datasets introduces further challenges, such as the curse of dimensionality, feature redundancy, and elevated computational demands. Conventional deep learning architectures—such as Convolutional Neural Networks (CNNs), Recurrent Neural Networks (RNNs), and hybrid CNN-LSTM frameworks—have been applied to pose- and video-based ASD detection tasks. While these approaches have achieved promising results, their effectiveness is often contingent upon access to large-scale training datasets and substantial computational resources. Consequently, their direct applicability to small-scale or resource-constrained clinical datasets, such as the one employed in this study, remains limited.

## 1.2 Major contributions

The primary objective of this study is to detect ASD in children using supervised ML classification algorithms in combination with nature-inspired optimization techniques. The supervised ML algorithms are employed to perform classification—determining whether a given individual is diagnosed with ASD or not—while the nature-inspired optimization algorithms are utilized for effective feature selection from the dataset. Both supervised learning methods and meta-heuristic optimization algorithms have demonstrated strong capabilities in handling high-dimensional and complex datasets, thereby enhancing predictive performance.

In particular, the objective of this work can also be framed as the detection of ASD from a three-dimensional walking video dataset of children. Walking represents one of the most fundamental motor skills in human development and carries the potential to reveal early indicators of ASD; thus, gait analysis can serve as a promising modality for diagnostic support. Building on this perspective, the present study leverages features extracted from 3D walking videos of children to address the ASD detection problem.

In addition to standard ML classification algorithms, we incorporate nature-inspired optimization algorithms for feature selection within high-dimensional datasets. To the best of our knowledge, the work presented here includes several methodological contributions not previously addressed in ASD detection research:

- Integration of nature-inspired optimization algorithms for feature selection and ranking of features using multiple ranking coefficients.
- Utilization of three-dimensional walking video data of children as the primary dataset for ASD detection.
- A comprehensive comparative study of various ML classification algorithms, feature-ranking coefficients, and nature-inspired optimization algorithms.

Through these contributions, the proposed methodology seeks to improve both the efficiency and accuracy of current ASD detection models, while simultaneously reducing the total computational cost associated with processing and classification. Thus, this research contributes to the growing body of work on ASD detection by demonstrating the potential synergy between ML-based classifiers and bio-inspired feature selection algorithms. The insights presented here not only establish a foundation for further developments in automated early detection systems but may also support advancements in timely intervention and treatment planning for individuals with ASD.

## 1.3 Problem statement

Through a novel methodology that integrates ML classification algorithms with nature-inspired optimization techniques for feature extraction, this study aims to contribute to the field of ASD detection.

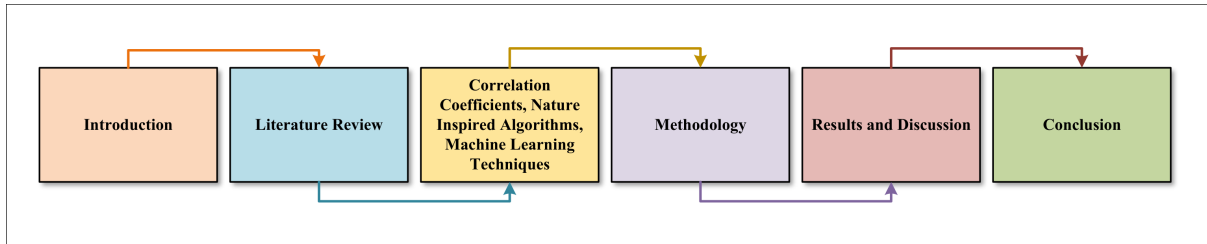


Fig. 1: Organization of the paper

Nature-inspired optimization algorithms have recently gained considerable attention for feature selection due to their ability to identify the most relevant features while significantly reducing overall computational cost. Furthermore, the incorporation of ranking coefficients within the proposed methodology provides an effective strategy for initializing the leading particles of the optimization algorithm, thereby enhancing efficiency and further reducing computation time.

#### 1.4 Organization of the paper

The remaining paper is organized as follows: Section 2 provides a comprehensive literature review of the concepts related to ASD detection using ML algorithms. Section 3 gives the preliminaries required for understanding the subsequent sections of the research paper. Section 4 presents the algorithm and methodology employed in this research paper. Section 5 describes the dataset specifications, data processing techniques, and feature extraction methods utilizing nature-inspired optimization algorithms. Section 5 also presents the performance evaluation metrics and results obtained for each algorithm combination. Finally, section 6 concludes the paper by summarizing the key findings and suggesting potential areas for future research.

## 2 Literature review

Early detection of ASD is of paramount importance to ensure timely and appropriate intervention for affected individuals. However, achieving high accuracy in ASD detection remains a significant challenge, requiring advanced assessment tools and specialized expertise. Recent advancements in the field include the following:

- Standardized ASD diagnostic instruments such as the Autism Diagnostic Observation Schedule (ADOS), Childhood Autism Rating Scale (CARS), and Autism Diagnostic Interview-Revised (ADI-R) have been developed to facilitate reliable identification of ASD in individuals [1, 2, 3, 4].
- Computerized technologies, including robotics, virtual reality, and computer gaming, have shown promising results in enhancing social communication skills among individuals diagnosed with ASD.
- Advances in machine learning and mathematical optimization techniques—such as Natural Language Processing (NLP), Long Short-Term Memory (LSTM) networks, autoencoders, and deep learning architectures—have demonstrated superior performance in ASD detection compared to traditional approaches, achieving significantly higher accuracy rates [1, 5, 4].
- The utilization of biological and physiological markers, including heart rate data and eye-gaze tracking, has gained attention recently as practical indicators for ASD detection. Notably, systems such as the Autonomous Social Orienting Training System (ASOTS), which employs a Response to Name (RTN) mechanism, are currently in use for diagnostic support [2, 3].

Table 1 summarizes some of the most recent advancements in ASD detection leveraging machine learning techniques. As demonstrated, computerized and algorithmic approaches have become increasingly prominent both in the detection and intervention of ASD. In particular, the effectiveness of nature-inspired optimization algorithms in selecting key features has been shown to reduce overall computational time while enhancing detection accuracy.

The primary focus of this research is to address several challenges present in recent advancements in ASD detection, specifically those related to handling high-dimensional datasets, effective feature extraction, and reduction of overall computational time. These challenges with existing methodologies can be summarized as follows:

Table 1: Literature Review of recently published research papers in related fields.

Year	Author	Aim	Dataset used	Methodology	Results	Limitations
2025	Shin et al. [6]	ASD detection using dual-stream deep learning	Gait 3D video movement dataset [7] of children.	Proposed CNN, Transformers, and hybrid CNN+Transformer model	Accuracy ranging from 93.2% to 95.4%;	Computationally expensive and not very reliable due to black-box nature.
2025	Zeraati and Davoodi [8]	ASD-GraphNet: graph learning for ASD diagnosis on fMRI data	Autism Brain Imaging Data Exchange (ABIDE) dataset.	Graph-based framework including mutual information + PCA and SHAP	Accuracy - 75.25%;	External dataset validation and perturbed/noisy data inclusion is required.
2024	Colonnese et al. [9]	Bimodal feature analysis with deep learning for ASD detection	Gait 3D video movement dataset [7] of children.	Proposed different architectures: LandNet, AngleNet, ConcatNet.	Accuracy ranging from 97.4% to 98.6%;	Computationally expensive and not very reliable due to black-box nature.
2024	Kalam et al. [10]	ML approach for identifying ASD from video	Gait 3D video movement dataset [7] of children.	Performed analysis using Random Forest + PCA for feature extraction	Accuracy - 95%;	Better method exists for classification accuracy.
2023	Henderson et al. [11]	Monocular Human Pose Estimation models	Gait 3D video movement dataset [7] of children.	Proposed CLIFF, VideoPose using PoseAug, and PSTMO	Accuracy ranging from 64.96% to 79.87%;	Better method exists for classification accuracy.
2022	Malathi and Kannan [12]	Adaptive Whale Optimization-based Support Vector Machine for Prediction of ASD	Child, Adult, and Adolescent ASD Dataset from UCI Machine Learning Website.	Adaptive Whale Optimization-based SVM is divided into 3 phases: Exploitation, Exploration, and Classification.	Accuracy for the dataset, Child - 90.753%; Adolescent - 90.385%; Adult - 89.347%;	Better algorithms already exist. Example: Modified Grasshopper Optimization algorithm.
2022	Sahu and Verma [13]	Classification of Autistic Spectrum Disorder Using Deep Neural Network with Particle Swarm Optimization	Child and Adolescent ASD Dataset from UCI Machine Learning Website.	Particle Swarm Algorithm (PSO) for feature selection and Multi-Layer Perceptron (MLP) and Deep Neural Network (DNN) for classification	Accuracy for the PSO-DNN model, Adolescent - 98.077%; Child - 100%;	Only can be applied to textual data. It is prone to different types of datasets, such as video datasets.
2022	Malathi and Kannan [14]	Robust Artificial Bee Colony Optimization-Based Classifier for Prediction of ASD	Child, Adult, and Adolescent ASD Dataset from UCI Machine Learning Website.	Robust Artificial Bee Colony Optimization (RABC) for feature selection and Decision Tree based Gradient Boosting (DTGB) for classification	Accuracy for the dataset, Child - 82.877%; Adolescent - 82.692%; Adult - 84.233%;	Better algorithms already exist. Example: Modified Grasshopper Optimization algorithm.
2021	Saranya and Anandan [15]	Autism Spectrum Prognosis using Worm Optimized Extreme Learning Machine (WOEM) Technique	Kaggle Dataset on Autism Spectrum Disorder.	Glow Worm Algorithm with Extreme Learning Machine (Single Hidden Layer)	Accuracy - 99%; Better results and faster than particle swarm Optimization algorithm	Only can be applied to textual data. It is prone to different types of datasets, such as video datasets.
2021	Elshoky et al. [16]	Machine Learning Techniques based on Feature Selection for Improving ASD	Child and Adult ASD Dataset from UCI Machine Learning Website.	Binary Firefly Feature Selection Algorithm was then applied to various ML algorithms for classification.	Accuracy - 100%; Binary Firefly for feature selection and Logistic Regression.	can only be applied to textual data. It is prone to different types of datasets, such as video datasets.
2021	Balakrishnan et al. [17]	Detecting Autism Spectrum Disorder with Sailfish Optimization	Child and Adult ASD Dataset from UCI Machine Learning Website.	Random Opposition-based Learning Sailfish Optimization (ROBL-SFO) with 10-fold cross-validation and SVM for classification	Accuracy for the dataset, Child - 97.30%; Adult - 94.20%; Efficiency increases by 3.07%.	Not validated for Adolescence dataset. No surety of good results in video/audio dataset.
2020	Goel et al. [18]	Modified Grasshopper Optimization Algorithm for detection of ASD	Child, Adult and Adolescent ASD Dataset from UCI Machine Learning Website.	Modified Grasshopper Optimization Algorithm for feature selection. Used 2-3 principal components and trained using Random Forest for classification.	Accuracy for the dataset, Child - 100%; Adolescent - 100%; Adult - 99.29%;	Convergence speed is slow for Grasshopper Optimization Algorithm, hence computational time is increased.
2020	Farrell et al. [19]	Combined Firefly Algorithm Random Forest (FARF) to Classify Autistic Spectrum Disorders	Child ASD Dataset from UCI Machine Learning Website.	Firefly algorithm for feature selection and Random Forest (RF) for classification	Accuracy - 94.32%; Better than RF with 90.78% accuracy.	Optimal number of Decision trees can't be found. Better algorithm already exists for ASD classification
2020	Li et al. [4]	Classifying ASD children with LSTM based on raw videos	Dataset consists of 272 children of primary and special ed. schools (Restricted Data)	Three three-layer Long Short-Term Memory Network is used for classification.	Accuracy - 93.4%	Feature extraction may reduce computation time and give satisfactory results.
2019	Abitha and Vennila [20]	Swarm-based Symmetrical Uncertainty Feature Selection method for ASD	Child ASD Dataset from UCI Machine Learning Website.	Combination of Symmetrical Uncertainty and PSO used for feature selection and Naive Bayes used for classification	Naive Bayes, Accuracy - 86.75%; Artificial Neural Networks, Accuracy - 83.53%;	Not validated for Adult and Adolescence dataset.
2018	Samad et al. [21]	Autism behavioural Markers in Spontaneous Facial, Visual, and Hand Movement Response Data	Dataset consists of volunteering basis humans (Restricted Data)	Movement of cursor and Eye gazing on the cursor (Response time analysis) for detection of ASD	Poor correlation between eye gaze and hand movement in ones who suffers ASD	Theoretical based paper which can be further improved by using Machine Learning approaches.

- The management of high-dimensional datasets remains a significant issue, as many contemporary ASD datasets consist of video and image data characterized by a large number of features. Such high dimensionality increases computational complexity, which can adversely affect both model performance and accuracy. This study aims to develop methods that facilitate efficient analysis and utilization of high-dimensional datasets, ultimately improving ASD detection accuracy.
- Feature extraction constitutes another critical challenge, as the selection of relevant and informative features directly impacts both accuracy and computational efficiency. Effective feature selection algorithms must be capable of identifying the most important features from vast feature spaces, thereby enhancing accuracy while reducing processing time.
- Computational time is a crucial concern, particularly given the urgent need for rapid results in medical applications. This research addresses this challenge by employing appropriate feature selection algorithms and correlation coefficients to identify initial leading particles for optimization-based feature selection, thereby significantly reducing the total computational time.

### 3 Preliminary

This section presents essential background information and fundamental concepts necessary for understanding the subsequent sections of this research paper. It provides detailed descriptions of various correlation coefficients, nature-inspired optimization algorithms, and supervised machine learning classification algorithms employed in this study.

#### 3.1 Correlation coefficients

In statistics, correlation provides a means to quantify the relationship between two different variables, which may be either random or deterministic. Correlation describes how a change in one variable corresponds to a change in another variable. It can be viewed as a representation of the monotonic association between two variables. In the case of positive correlation, changes in both variables occur in the same direction, whereas in negative correlation, the changes occur in opposite directions [22].

##### 3.1.1 Pearson correlation coefficient

The Pearson Correlation Coefficient (PCC), denoted by  $\rho$ , measures the linear correlation between two variables and ranges between  $[-1, 1]$ , where positive and negative values indicate positive and negative correlations, respectively, and zero indicates no correlation. PCC quantifies both the strength and direction of the linear relationship and can be used for selecting relevant features or important observations from a dataset [23].

The PCC between variables  $x$  and  $y$  is computed as

$$\rho_{x,y} = \frac{\text{cov}(x,y)}{\sigma_x \sigma_y} \quad (1)$$

where  $\text{cov}(x,y)$  represents the covariance between variables  $x$  and  $y$ , and  $\sigma_i$  denotes the standard deviation of the  $i^{\text{th}}$  variable.

##### 3.1.2 Spearman correlation coefficient

The Spearman Correlation Coefficient (SCC), denoted by  $r_S$ , also measures the degree of correlation between two variables. Unlike PCC, SCC is less sensitive to outliers and does not assume a linear relationship, making it preferable when dealing with ordinal data or datasets with potential outliers [23].

SCC between variables  $x$  and  $y$  is calculated as

$$r_S = \rho_{R_x, R_y} \quad (2)$$

where  $R_x$  and  $R_y$  denote the ranks of variables  $x$  and  $y$ , respectively.

### 3.1.3 Relief ranking coefficient

The Relief ranking algorithm is an iterative feature weighting method that evaluates the relevance of each feature within a dataset. During each iteration, the algorithm selects instances that are close within the feature space and updates the feature weights accordingly. These weights, known as relief ranking coefficients, help identify the most informative attributes and rank them accordingly. The Relief algorithm is particularly effective for handling high-dimensional datasets [24].

The weight vector update for the Relief algorithm is given by

$$W_i = W_i - (x_i - \text{nearHit}_i)^2 + (x_i - \text{nearMiss}_i)^2 \quad (3)$$

where  $x$  is the feature vector and  $W_i$  is the weight for the  $i^{\text{th}}$  attribute.

## 3.2 Nature-inspired algorithms

Nature-inspired algorithms are optimization methods used for a variety of tasks, including optimization, feature selection, and more. Also known as bio-inspired algorithms, they are derived from natural systems and phenomena. These algorithms imitate the dynamic behaviors observed in nature, such as evolutionary processes, swarm intelligence, and genetic inheritance. By leveraging these natural principles, nature-inspired algorithms effectively solve complex and challenging optimization problems [25, 26, 27].

### 3.2.1 Gravitational Search Algorithm

The Gravitational Search Algorithm (GSA) is a nature-inspired optimization technique based on Newton's law of gravitation. In GSA, each feature is modeled as an object with a corresponding mass, and all objects attract each other via gravitational forces, with heavier masses exerting stronger attraction. This mechanism enables GSA to explore the entire solution space efficiently and converge to an optimal solution. GSA has proven to be a powerful optimization approach for solving complex problems [28]. Newton's law of gravitation is mathematically expressed as

$$F = \sum_{i=1}^{n-1} \sum_{j=i+1}^n G \frac{M_i M_j}{R_{i,j}^2} \quad \text{and} \quad a_i = \frac{F}{M_i} \quad (4)$$

where  $n$  is the total number of objects,  $G$  represents the gravitational constant,  $F$  denotes the total gravitational force,  $R_{i,j}$  is the distance between the  $i^{\text{th}}$  and  $j^{\text{th}}$  objects,  $M_i$  is the mass of the  $i^{\text{th}}$  object, and  $a_i$  is the acceleration of the  $i^{\text{th}}$  object.

### 3.2.2 Binary Bat Algorithm

The Bat Algorithm (BA) is inspired by the echolocation behavior of bats, which use ultrasonic high-frequency sound pulses to navigate and locate prey at night. Bats analyze the reflected echoes to infer information about their surroundings, even in complete darkness. The Binary Bat Algorithm (BBA) is a binary adaptation of the original BA, employing the same principle of echolocation for discrete optimization problems [29]. The transfer and position update functions in BBA are defined as follows:

$$S(v_i^k(t)) = \frac{1}{1 + e^{-v_i^k(t)}} \quad (5)$$

$$x_i^k(t+1) = \begin{cases} 0, & \text{if rand} < S(v_i^k(t+1)) \\ 1, & \text{if rand} \geq S(v_i^k(t+1)) \end{cases} \quad (6)$$

where  $x_i^k(t)$  and  $v_i^k(t)$  represent the position and velocity vectors, respectively, of the  $i^{\text{th}}$  particle at iteration  $t$  in the  $k^{\text{th}}$  dimension.

### 3.2.3 Cuckoo Search Algorithm

The Cuckoo Search Algorithm (CS) is a nature-inspired optimization algorithm based on the brood parasitic breeding behavior of cuckoo birds, which lay their eggs in the nests of other host birds. CS incorporates Lévy flights, representing random walks with step sizes following a heavy-tailed probability distribution, enabling efficient exploration of the search space and effective escaping from local optima.

Consequently, CS demonstrates superior performance compared to many other swarm intelligence algorithms [30]. The nonlinear update system in CS is expressed as

$$x_i^{t+1} = x_i^t + \alpha L(s, \lambda) \quad (7)$$

$$L(s, \lambda) \sim \frac{\lambda \Gamma(\lambda) \sin\left(\frac{\pi\lambda}{2}\right)}{\pi} \frac{1}{s^{1+\lambda}}, \quad (s > 0) \quad (8)$$

where  $\alpha > 0$  is a user-defined step size scaling factor.

### 3.2.4 Genetic Algorithm

The Genetic Algorithm (GA) is an evolutionary optimization technique inspired by Darwin's theory of natural selection and the survival of the fittest principle. GA operates iteratively, where the fittest offspring are selected in each generation to produce subsequent generations. Each iteration corresponds to a population generation, consisting of the following stages:

1. **Selection:** Dominant parents are chosen from the population based on fitness, where selection is guided by survival probability and expected fitness, aiming to identify the best features for reproduction.
2. **Crossover:** This process generates offspring by combining the genetic information of selected parents. The specific crossover methods may vary depending on application needs.
3. **Repeat the Process:** The selection and crossover steps are repeated across multiple generations to progressively improve the population. If improvement stagnates over generations, mutation is introduced.
4. **Mutation:** Used sparingly, mutation introduces random changes in offspring to maintain genetic diversity and help avoid local optima when evolutionary progress stagnates.

GA is one of the foundational nature-inspired optimization algorithms. The selection and crossover phases replicate natural selection and genetic recombination, facilitating the survival and propagation of advantageous traits. Through iterative population improvement, GA extensively explores the solution space to identify optimal or near-optimal solutions.

### 3.2.5 Grey Wolf Optimization Algorithm

Grey Wolf Optimization (GWO) is a nature-inspired algorithm modeled after the hunting behavior of grey wolves, which organize in a hierarchical social structure consisting of four groups:  $\alpha$ ,  $\beta$ ,  $\delta$ , and  $\omega$ , where  $\alpha$  represents the dominant group and  $\omega$  the lowest rank [31]. While GWO is more complex to implement compared to similar algorithms, it frequently achieves superior results due to its diverse parameter set. The mathematical model of GWO is described as follows:

$$D = |CX_p(t) - X(t)|\omega \quad (9)$$

$$X(t+1) = X_p(t) - AD \quad (10)$$

$$A = 2ar_1 - a \quad (11)$$

$$C = 2r_2 \quad (12)$$

$$a = 2 - \frac{2t}{T_{max}} \quad (13)$$

$$\begin{cases} D_\alpha = |CX_\alpha - X| \\ D_\beta = |CX_\beta - X| \\ D_\delta = |CX_\delta - X| \end{cases} \quad (14)$$

$$\begin{cases} X_1 = X_\alpha - A_1 D_\alpha \\ X_2 = X_\beta - A_2 D_\beta \\ X_3 = X_\delta - A_3 D_\delta \end{cases} \quad (15)$$

$$X(t+1) = \frac{X_1 + X_2 + X_3}{3} \quad (16)$$

where  $X_p(t)$  and  $X(t)$  are the prey and grey wolf position vectors at iteration  $t$ ,  $r_1, r_2$  are random vectors in  $[0, 1]$ ,  $T_{max}$  is the maximum number of iterations,  $D_i$  is the distance between the wolf and the  $i^{th}$  leading wolf, and  $X_i$  for  $i \in \{\alpha, \beta, \delta\}$  denote the position vectors of the top three wolves guiding the search.

### 3.2.6 Particle Swarm Optimization Algorithm

Particle Swarm Optimization (PSO) is a metaheuristic algorithm inspired by the swarming behavior of birds and fish. In PSO, each particle moves through the solution space by updating its velocity based on its own experience and the experience of the entire swarm. The velocity update is influenced by a global best position and the particle's personal best position, guiding the swarm toward optimal solutions. Iterative updates of velocity and position enable the swarm to converge to the global optimum. The velocity and position of the  $i^{th}$  particle are updated as follows:

$$v_i^{t+1} = v_i^t + \alpha\epsilon_1(g^* - x_i^t) + \beta\epsilon_2(x_i^* - x_i^t) \quad (17)$$

$$x_i^{t+1} = x_i^t + v_i^{t+1} \quad (18)$$

where  $x_i^t$  and  $v_i^t$  are the position and velocity vectors of the  $i^{th}$  particle at iteration  $t$ ,  $g^*$  is the global best-known position,  $x_i^*$  is the personal best position of particle  $i$ ,  $\epsilon_1, \epsilon_2$  are independent random vectors uniformly distributed in  $[0, 1]$ , and  $\alpha, \beta$  are acceleration coefficients controlling the influence of the social and cognitive components, respectively.

### 3.2.7 Whale Optimization Algorithm

The Whale Optimization Algorithm (WOA) is inspired by the bubble-net hunting strategy of humpback whales. Whales create spiraling bubbles to concentrate prey into smaller areas before capture. Analogously, WOA progressively narrows the search area around the best solutions, enabling exploitation of the most promising regions of the search space [32]. The mathematical model of WOA is described by the following equations:

$$D = |CX^*(t) - X(t)| \quad (19)$$

$$X(t+1) = X^*(t) - AD \quad (20)$$

$$A = 2a \cdot \text{rand} - a \quad (21)$$

$$C = 2 \cdot \text{rand} \quad (22)$$

$$a = 2 - \frac{2t}{T_{max}} \quad (23)$$

$$X(t+1) = D'e^{bl} \cos(2\pi l) + X^*(t) \quad (24)$$

$$D' = |X^*(t) - X(t)| \quad (25)$$

where  $t$  is the current iteration number,  $X^*(t)$  is the current best solution (prey position),  $X(t)$  is the position vector,  $a$  and  $b$  are constants,  $\text{rand}$  is a random number in  $[0, 1]$ ,  $T_{max}$  is the maximum number of iterations,  $D'$  is the distance between the whale and the prey,  $l$  is a random number in  $[-1, 1]$ , and the exponential-cosine term models the logarithmic spiral path of the whale's hunting maneuver. The condition  $|A| \geq 1$  governs the exploration phase of the algorithm.

## 3.3 Supervised Machine Learning Algorithms

Supervised ML algorithms operate on labeled input-output data pairs. These algorithms aim to learn a mapping function or transformation that associates an input variable  $x$  with its corresponding output variable  $y$ . Being data-driven, supervised ML relies entirely on the quality and accuracy of the provided data for effective learning. Once trained, the mapping function enables prediction of output values for unseen inputs, generally achieving higher accuracy than unsupervised learning methods [33, 34].

### 3.3.1 Support Vector Machine

Support Vector Machines (SVMs) are supervised ML algorithms applicable to both classification and regression tasks. For classification, SVM constructs an optimal hyperplane that separates data points belonging to different classes, where the hyperplane's dimension corresponds to the number of features in the dataset.

### 3.3.2 K-Nearest Neighbors

K-Nearest Neighbors (KNN) is a simple yet effective supervised classification algorithm. It classifies an instance based on the majority class among its  $K$  nearest neighbors, determined through Euclidean distance minimization.

### 3.3.3 Random Forest

Random Forest (RF) is a supervised ensemble learning algorithm that builds a large collection of decision trees, either in sequence or in parallel, hence the name. Each tree is trained on a random subset of the data and features, contributing to a robust aggregated prediction.

These fundamental supervised ML concepts form the basis for the methodologies proposed in subsequent sections of this paper. The integration of these algorithms with feature selection techniques aims to significantly reduce computational time while improving predictive accuracy.

## 4 Methodology

To achieve high accuracy in ASD classification, a robust methodological pipeline is designed, consisting of systematic data pre-processing, correlation-based feature ranking, nature-inspired feature selection, model training with nested cross-validation, and comprehensive evaluation.

### 4.1 Data Pre-processing

The data pre-processing step in the proposed methodology is the first and most important step required to ensure the quality of the dataset. Data pre-processing consists of several minor steps, including data cleaning and null value removal. Data cleaning involved the removal of unnecessary data in the dataset, for example, variance and standard deviation represent the same values. After data cleaning, the dimension of the dataset is reduced to some extent. There are no null values present in our dataset, hence the removal of null value step is not required. Finally, after the data pre-processing step, our dataset was left with 860 feature columns out of 1259 feature columns.

### 4.2 Main Methodology

#### 4.2.1 Feature Ranking

To prioritize informative biomarkers, three correlation-based criteria rank features, PCC, SCC, and Relief. This multi-perspective ranking highlights the most influential features as leaders for the subsequent nature-inspired optimizers.

#### 4.2.2 Feature Extraction

Nature-inspired metaheuristic algorithms are deployed to extract an optimal subset of features. For all optimizers, the initial population is seeded using the top-ranked features, accelerating convergence. The process maintains a balance between classification accuracy (80% weight) and dimensionality reduction (20% weight) in the fitness function. We considered seven benchmarked algorithms for this, namely, BBA, CS, GA, GSA, GWO, PSO, and WOA. This step dramatically reduces dataset dimensionality, thereby minimizing computational complexity.

#### 4.2.3 Classification

Selected feature sets are evaluated using three of the most famous machine learning classifiers, KNN with  $k = 5$ , RF with 100 trees, and SVM with RBF kernel. Classifiers are trained and validated on optimized feature sets for ASD status prediction.

#### 4.2.4 Nested Cross-Validation, Training and Testing

A rigorous nested cross-validation strategy is adopted to prevent overfitting and fine-tune hyperparameters. The outer 5-fold stratified Cross-Validation (CV) assesses model performance generalization. For each outer fold, feature selection and an inner 3-fold CV are performed for classifier selection and tuning.

Within each fold, the optimizer uses a population of 30 and a maximum 100 iterations. Additionally, a standard 80:20 train-test split is maintained, with 20% held out for validation. All hyperparameter searches employ scikit-learn’s `GridSearchCV` framework.

### 4.3 Model Evaluation

Each combination of ranking method, feature selector, and classifier is evaluated on multiple metrics, including Accuracy, Recall, Precision, and F1-score. Along with these metrics, Confusion matrix analysis, average feature count, and runtime per configuration are also considered for analysis.

Pairwise statistical tests (paired *t*-test, Wilcoxon signed-rank) are also performed across nature-inspired methods to assess the significance of observed improvements. Notably, the combination of Relief, GSA, and RF achieves 100% accuracy with 380 features, while Relief, CS, and RF provide 96.88% accuracy with only 4 features, underscoring the strength of dimensionality-driven optimization.

### 4.4 Algorithm Analysis

Algorithm 1 is designed to handle textual data inputs, which makes it inherently suitable for processing modalities such as video, image, and textual datasets (Section 5.1). This suitability arises from the conversion of raw video or image data into numerical textual representations, enabled by pixel-wise or body landmark analyses. For instance, the original gait video, of which a still frame is shown in Fig. 2a, captures an individual’s motion. Specific points selected on the body, illustrated in Fig. 2b, are tracked over time. The trajectories of these points, given by Fig. 2c, generate the textual dataset used for subsequent analysis and algorithmic processing.

Through feature extraction on this textual data, irrelevant or redundant features are systematically removed to improve computational efficiency and model generalization. The resulting curated dataset forms the basis of the proposed methodology for ASD prediction and optimal model selection.

For example, from Table 4, we can see that the combination of the Relief correlation coefficient, Cuckoo Search (CS) for feature selection, and Random Forest (RF) classifier yields near-optimal performance using only four features with an accuracy of 96.875%. These features are,

1. **mean-x-FootRight**: The mean position of the right foot along the x-axis (horizontal).
2. **std FoRTThR**: The correlation between the right foot and right thumb.
3. **std HaRTKeR**: The correlation between the right hand and right knee.
4. **std KeLTSb**: The standard deviation of the left knee.

Three out of these four features explicitly measure deviations or variability from mean body point trajectories, aligning with clinical observations that ASD commonly involves altered motor coordination and neuromotor development. This observation theoretically supports the algorithm’s focus on dynamic and variable features rather than static averages, thereby improving discriminative power.

From an algorithmic perspective, the integration of multi-criteria correlation ranking with nature-inspired feature selection methods enables a balanced trade-off between dimensionality reduction and prediction accuracy. The 80% weighting towards accuracy ensures that selected features robustly characterize ASD-related patterns, while the 20% weighting for feature reduction guards against overfitting and excessive model complexity. Thus, the theoretically informed feature subset and the robust nature-inspired algorithms and classifier algorithm combination identified in this methodology not only facilitate accurate ASD prediction but also promote interpretable models driven by physiologically meaningful markers.

## 5 Result analysis and visualization

The result analysis section of this research paper covers various analyses of combinations. Initially, a study of the dataset is done, which provides in-depth knowledge of the data that is used in our methodology. After this, the performance of various combinations of algorithms is evaluated using confusion matrices. Finally, we provide a full explanation of the outcomes we got in the previous steps. Adding up this, these evaluations give us the final performance, statistical analysis, and significance of our methodology required for future research and applications.

---

**Algorithm 1:** Proposed Methodology Pipeline

---

**Data:** Dataset  $D \in \mathbb{R}^{m \times n}$  with  $m$  samples,  $n$  features; target labels  $y \in \mathbb{R}^m$

**Result:** Performance statistics of classifiers, selected feature subsets, runtime logs, and statistical comparisons

```
1 Initialize: FeatureMethods  $\leftarrow$  {PCC, SCC, Relief};
2 NatureAlgos  $\leftarrow$  {BBA, CS, GA, GSA, GWO, PSO, WOA};
3 Classifiers  $\leftarrow$  {KNN, RF, SVM};
4 foreach corr  $\in$  FeatureMethods do
5   Compute feature ranking scores  $S_{corr}(D, y)$ ;
6   Initialize the leading particle for NatureAlgo;
7   foreach NatureAlgo  $\in$  NatureAlgos do
8     foreach clf  $\in$  Classifiers do
9       Set up outer stratified  $K$ -fold CV ( $K=5$ );
10      Accuracies  $\leftarrow$  []; FeatureCounts  $\leftarrow$  []; Times  $\leftarrow$  [];
11      foreach (train_idx, val_idx)  $\in$  outer CV splits do
12         $D_{tr}, y_{tr} \leftarrow D[\text{train\_idx}], y[\text{train\_idx}]$ ;
13         $D_{val}, y_{val} \leftarrow D[\text{val\_idx}], y[\text{val\_idx}]$ ;
14        Run optimizer NatureAlgo with population size 30 and 100 iterations on  $(D_{tr}, y_{tr})$ ;
15        Obtain binary feature mask  $M \in \{0, 1\}^n$ ;
16        if  $\sum M = 0$  then
17          continue to next fold
18         $D_{tr,fs}, D_{val,fs} \leftarrow$  select features in  $M$ ;
19        FeatureCounts  $\leftarrow$  FeatureCounts  $\cup \{\|M\|_1\}$ ;
20        Set up stratified inner  $L$ -fold CV ( $L=3$ );
21        Perform GridSearchCV on  $clf$  hyperparameters with  $(D_{tr,fs}, y_{tr})$ ;
22        Let  $clf^*$  = best estimator from tuning;
23         $\hat{y}_{val} \leftarrow clf^*(D_{val,fs})$ ;
24        Accuracies  $\leftarrow$  Accuracies  $\cup \{\text{accuracy}(y_{val}, \hat{y}_{val})\}$ ;
25        Record runtime for feature selection and inner CV in Times;
26      if Accuracies  $\neq$  [] then
27        Compute  $\mu_{acc}, \sigma_{acc}^2, 95\%$  CI from Accuracies;
28        Compute precision, recall, F1-score, and confusion matrix;
29        Store metrics, mean feature count, and average runtimes into
        Results[corr][NatureAlgo][clf];
30 Statistical Analysis;
31 foreach corr  $\in$  FeatureMethods do
32   foreach clf  $\in$  Classifiers do
33     Compare accuracies of all pairs of NatureAlgos  $(w_1, w_2)$  on common folds;
34     Apply paired  $t$ -test and Wilcoxon signed-rank test between  $(Acc_{w_1}, Acc_{w_2})$ ;
35     Store  $p$ -values in Stats[corr][clf];
36 Output: Results, Runtimes, and Stats.
```

---

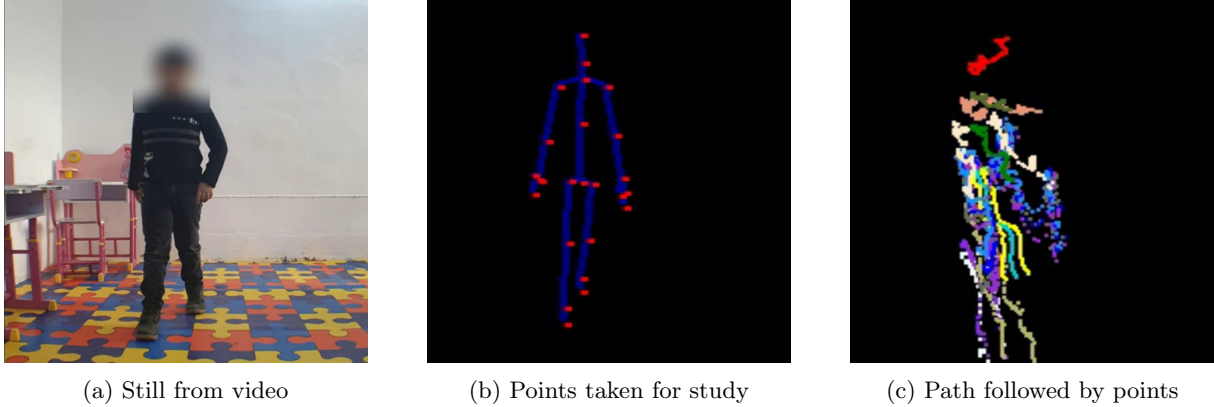


Fig. 2: 3D Videos of children walking towards the camera

## 5.1 Dataset description

In order to utilize a video dataset for classification, we must have to transform the dataset into textual data. This is done through analysis of joint motions along all three axes and determining standard deviation as well as variance. Angular deviation of some of the joints and other physical parameters are also extracted as textual data. These extracted features come out to be very useful in determining ASD in an individual, as they determine walking movement patterns, and ASD affects them very severely.

The dataset used in our research is “*Three-Dimensional Dataset Combining Gait and Full Body Movement of Children with Autism Spectrum Disorders Collected by Kinect v2 Camera Dataset*” [7], which is a publicly available dataset. A total of 100 Children are studied in the video dataset, 50 of whom are typical development, and the remaining 50 with ASD detected. A total of 1259 features are initially present in the extracted textual dataset.

Table 2 shows concise data in the given dataset, which includes the number of children tested for creation of the dataset, the number of data cases present in the given dataset, and the total number of missing values (nil/NA values). Table 3 shows all of the features extracted from the 3D walking video dataset, presented with their physical units and the total number of features belonging to that particular set of attributes. Physical units can be used for the data cleaning process in the data pre-processing step in our proposed methodology.

Table 2: General Dataset Description

Data Cases/ Children	Typical Development	Autism Spectrum Disorder	Total
Number of Children	50	50	100
Number of Data Cases	400	400	800
Missing Values	Nil	Nil	Nil

## 5.2 Performance/ Evaluation metrics

In this research work, we evaluated the performance of the model (combination of algorithms) using confusion matrices. A confusion matrix is used to describe performance, which encompasses various variables, including True Positive, False Positive, True Negative, and False Negative [16]. These matrices give in-depth knowledge of the model. Hence, the evaluation of the classification model is done using test accuracy, recall, precision, and F1 score.

## 5.3 Results

All the experiments are performed on an Intel i9-14900K CPU with a 3.20GHz frequency, 32GB RAM, and 32 cores. Base codes for implementation (Base implementation of nature-inspired algorithms for feature selection and Relief ranking coefficient) are adapted from the Py\_FS Python package [35] (Base implementation of nature-inspired algorithms for feature selection and Relief ranking coefficient) and implemented with Python 3.10.13. All parameters for the nature-inspired algorithms were set to their default values as specified in the Py\_FS Python package.

Table 3: Features included in dataset (.xlsx extracted from .avi) [7]

Abbreviation	Description	Type	Unit	Features
mean-coordination-Joint	Mean of x, y, and z coordination of 25 body joints	Floating-point	m	75
variance-coordination-Joint	Variance of x, y, and z coordination of 25 body joints	Floating-point	m2	75
std-coordination-Joint	Standard deviation of x, y, and z coordination of 25 body joints	Floating-point	m	75
mean Angle	Mean of 18 angles between body joints	Floating-point	deg	18
variance Angle	Variance of 18 angles between body joints	Floating-point	deg2	18
std Angle	Standard deviation of 18 angles between body joints	Floating-point	deg	18
mean joint1 T Joint2	Mean of distance between body joints	Floating-point	m	24
variance joint1 T Joint2	Variance of distance between body joints	Floating-point	m2	24
std joint1 T Joint2	Standard deviation of distance between body joints	Floating-point	m	24
Mean Joint TGr	Mean of distance between Joints and ground	Floating-point	m	282
variance Joint TGr	Variance of distance between Joints and ground	Floating-point	m2	282
std Joint1 TGr	Standard deviation of distance between Joints and ground	Floating-point	m	282
Rom Joint coordination	Range of movement of 25 joint on x and y coordination	Floating-point	m	50
MaxStLe	Maximum stride length	Floating-point	m	1
MaxStWi	Maximum stride width	Floating-point	m	1
StrLe	Stride length	Floating-point	m	1
GaCT	Gait cycle time	Time	ms	1
StaT	Stance time	Time	ms	1
SwiT	Swing time	Time	ms	1
Velocity	Velocity	Floating-point	m/s	1
HaTiLPos	Hand Tip left position relative to SpanBase	Binary (0, 1)	-	1
HaTiRPos	Hand Tip Right position relative to SpanBase	Binary (0, 1)	-	1
MaxDBFE and MinDBFE	Maximum and minimum distance between feet	Floating-point	m	2
Threshold	Using in extract one gait cycle = average of distance between feet	Floating-point	m	1
Total Number of Features	-	-	-	1259

After comprehensive evaluation of various combinations involving correlation coefficients, nature-inspired optimization algorithms for feature selection, and supervised machine learning classifiers (provided in **Appendix**), we identified that the combination of the GSA and RF yielded the highest classification accuracy of 100%. This optimal configuration employed the Relief ranking coefficient and selected 380 features. Significantly, among all tested combinations, this (Relief, GSA, RF) setup uniquely achieved perfect accuracy while simultaneously reducing features by 69.817% in the best case. If the priority shifts towards maximal feature reduction without placing paramount emphasis on attaining perfect accuracy, the combination of Relief coefficient, CS optimizer, and Random Forest classifier offers a notable alternative. This setup achieved an accuracy of 96.875% using only 4 features out of a total of 1259, corresponding to an exceptional feature reduction of 99.68% in the best case. For scenarios where computational efficiency and timing are critical, the combination of SCC, GA, and the KNN classifier stands out. This trio delivered an accuracy of 98.75% using 399 features with a runtime of merely 5 seconds. Remarkably, this runtime is reduced by 87.18% compared to the (Relief, GSA, RF) combination and by 85.2% relative to the (Relief, CS, RF) setup. Hence, depending on specific requirements - whether prioritizing accuracy, feature reduction, or computational efficiency - these three options provide flexible choices. Table 6 summarizes these key results for ease of comparison.

The average test accuracy analysis is visually represented using the histogram shown in Fig. 3, where different colors correspond to various nature-inspired optimization algorithms. The histogram is divided into two sections, highlighting the performances of different classifiers and feature ranking coefficients utilized during evaluation. It is evident from the histogram that the SVM consistently performs the worst across all combinations of ranking coefficients and classifiers, whereas the Relief ranking coefficient yields the best results overall. It is important to note that these accuracies represent average values, hence, for a more comprehensive understanding of model generalizability, one must also consider the results presented in Fig. 5 and Fig. 6. Furthermore, the pie charts depicted in Fig. 4 illustrate the mean number of features selected for each combination, while Fig. 7 represents the feature importance scores used for initial particle selection.

Fig. 5 depicts the nested cross-validation accuracy trends achieved by various nature-inspired optimization algorithms across the feature ranking coefficients. Each subplot corresponds to a different ranking coefficient, with multiple colored lines representing distinct classifier algorithms. Among all optimizers, the GSA demonstrated the smallest standard deviation and narrowest confidence intervals in accuracy, particularly when paired with the Relief ranking coefficient and the RF classifier. Both KNN and RF classifiers showed minimal fluctuations in accuracy over different data splits for most optimizers, indicating a robust feature selection pipeline and strong classifier generalization. Additionally, the GWO combined with the SCC ranking coefficient and RF classifier also exhibited low variability and tight accuracy intervals. These observations suggest multiple viable model configurations, allowing prac-

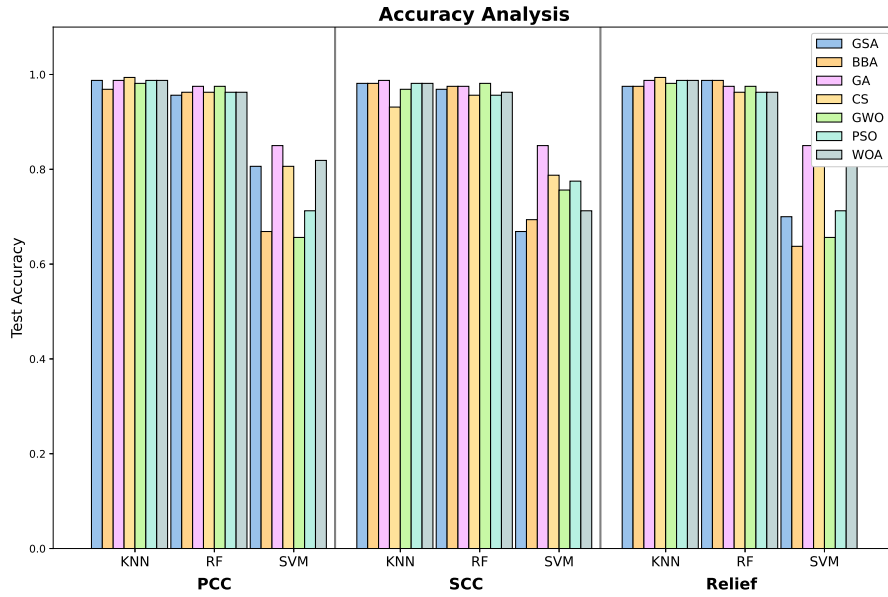
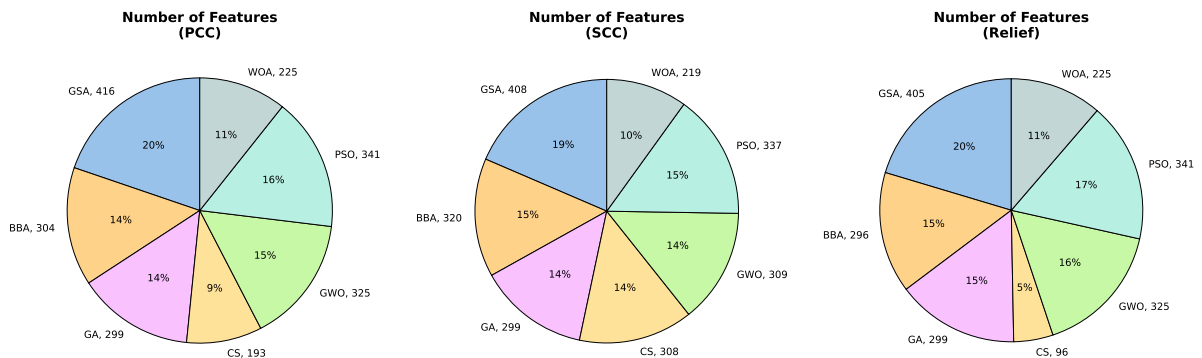


Fig. 3: Avg. test accuracy analysis of various combinations of feature extraction and classification algorithms



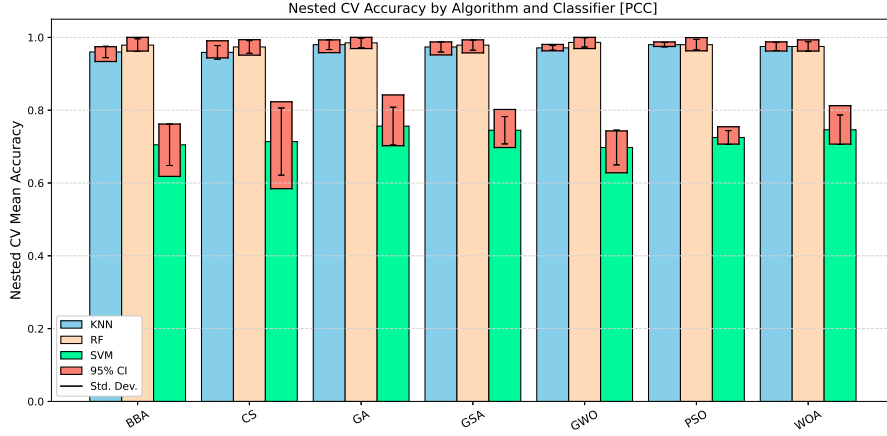
(a) Mean feature count for PCC      (b) Mean feature count for SCC      (c) Mean feature count for Relief

Fig. 4: Feature analysis of various nature-inspired algorithms

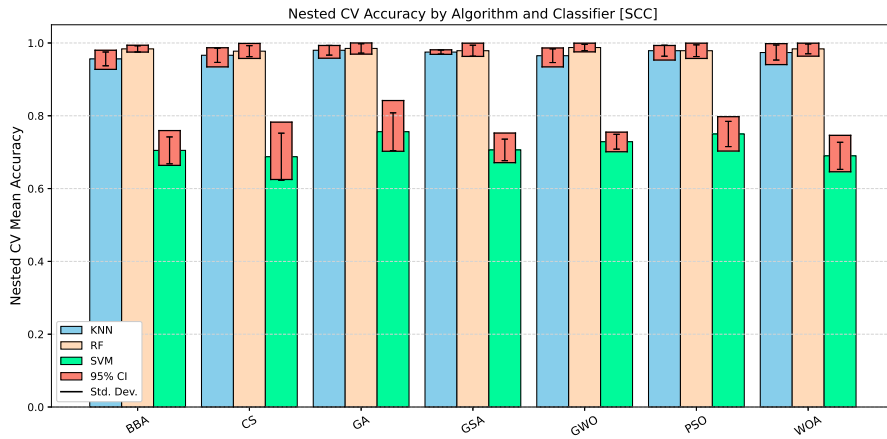
titioners to select models based on desired characteristics such as accuracy, stability, or computational efficiency. Fig. 6 visualizes the outer accuracy performance statistics across the folds for each combination of nature-inspired optimization algorithms and classifier, across all feature selection methods. Each subplot corresponds to a specific ranking approach, providing a direct comparative view of their impact. Across all plots, the RF classifier consistently. Notably, the accuracy remains high for virtually all nature algorithms, demonstrating the effectiveness of the pipeline’s stratified cross-validation and feature optimization.

## 5.4 Comparison with existing methods

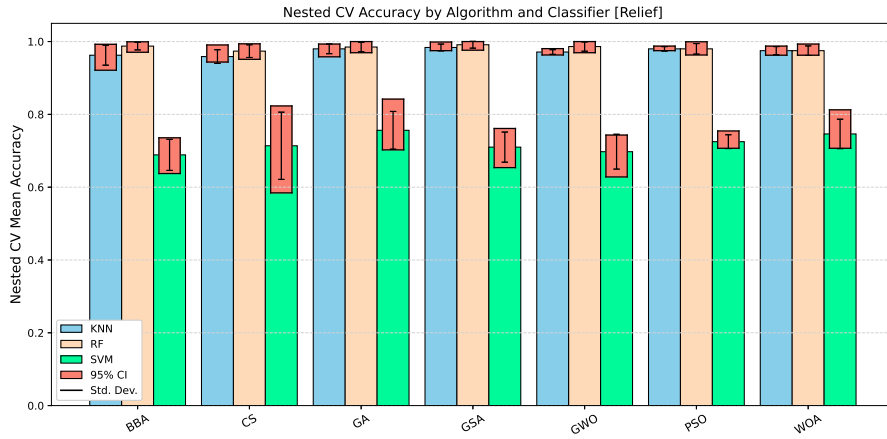
Comparisons are done with state-of-the-art methods, namely, Bimodal feature analysis with deep learning for autism spectrum disorder detection [9], Machine Learning Approach for Identification of Autism Spectrum Disorder from Video Using OpenPose [10], and Autism Spectrum Disorder Detection Using Skeleton-Based Body Movement Analysis via Dual-Stream Deep Learning [6]. The results presented in Table 5 clearly demonstrate the efficacy of the proposed Relief + GSA + RF framework in comparison with existing state-of-the-art approaches for ASD detection. Notably, while ConcatNet [9], among the bimodal fusion architectures, attained a strong performance with an accuracy of 0.986, the proposed method surpassed this benchmark by achieving an accuracy of 0.991, thereby establishing a new performance ceiling within this domain. Unimodal video-based methods, including Random Forest with



(a) Nested CV accuracy analysis using PCC



(b) Nested CV accuracy analysis using SCC



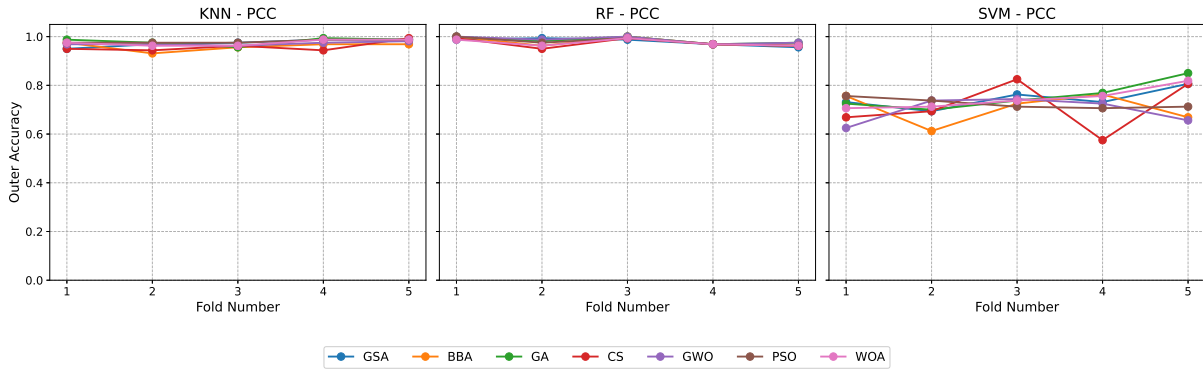
(c) Nested CV accuracy analysis using Relief

Fig. 5: Nested Cross-Validation Accuracy Analysis with 95% Confidence Interval and Standard Deviation

Table 4: Best Results obtained out of all the test runs

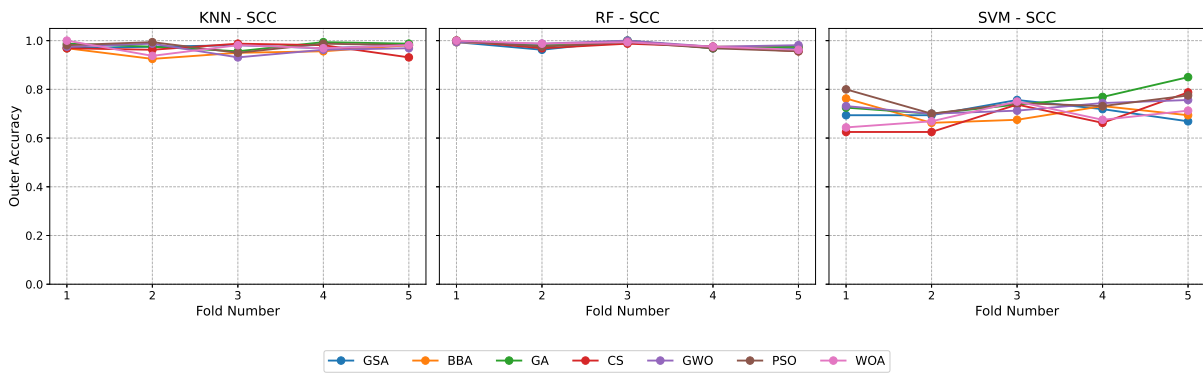
Combination of Algorithms	Accuracy	Time (s)	Avg. Features	Feature Reduction
Relief + GSA + RF	<b>100%</b>	≈ 39	380	69.81%
Relief + CS + RF	96.875%	≈ 27	<b>4</b>	<b>99.68%</b>
SCC + GA + KNN	98.75%	≈ <b>5</b>	399	68.31%

**Outer Accuracy across folds for PCC**



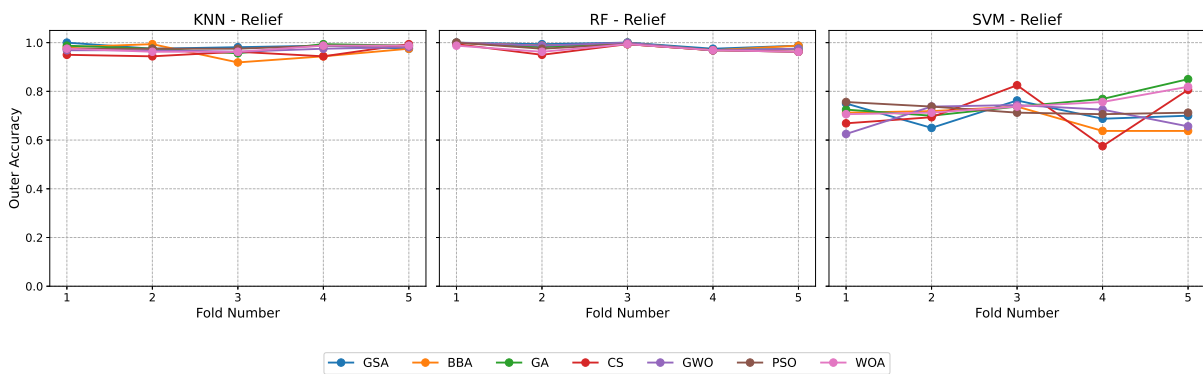
(a) Pearson Correlation Coefficient

**Outer Accuracy across folds for SCC**



(b) Spearman Correlation Coefficient

**Outer Accuracy across folds for Relief**



(c) Relief Ranking Coefficient

Fig. 6: Analysis of outer accuracy across the folds during training

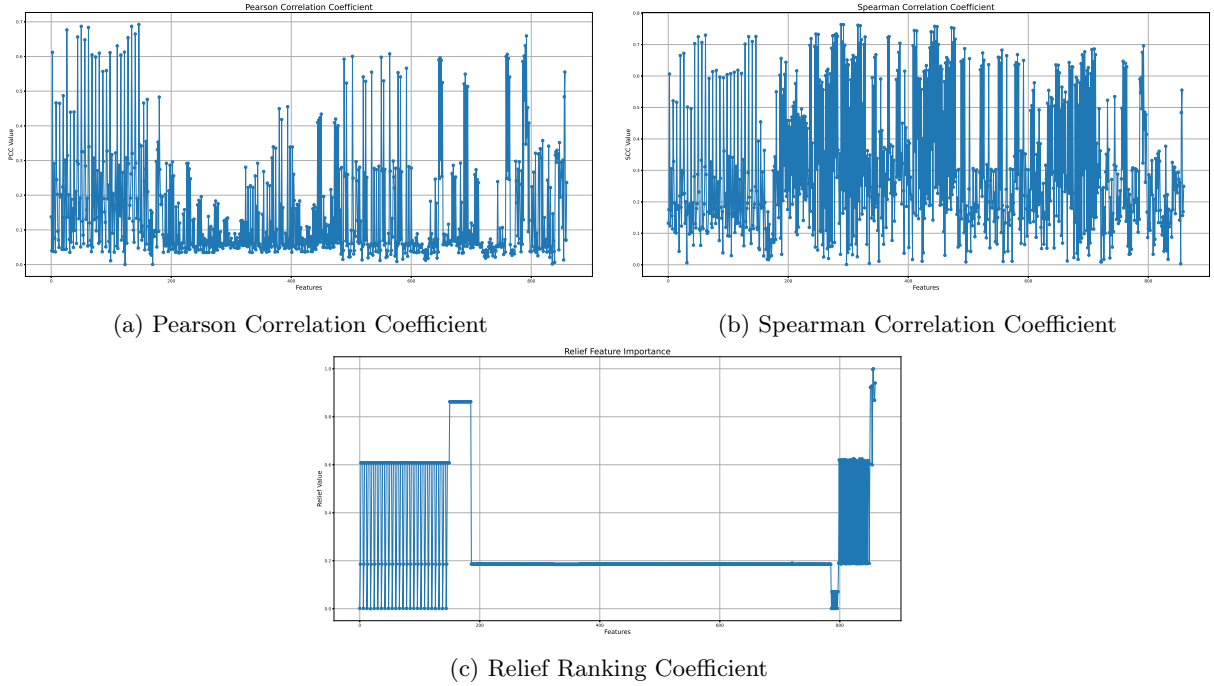


Fig. 7: Feature Importance Values

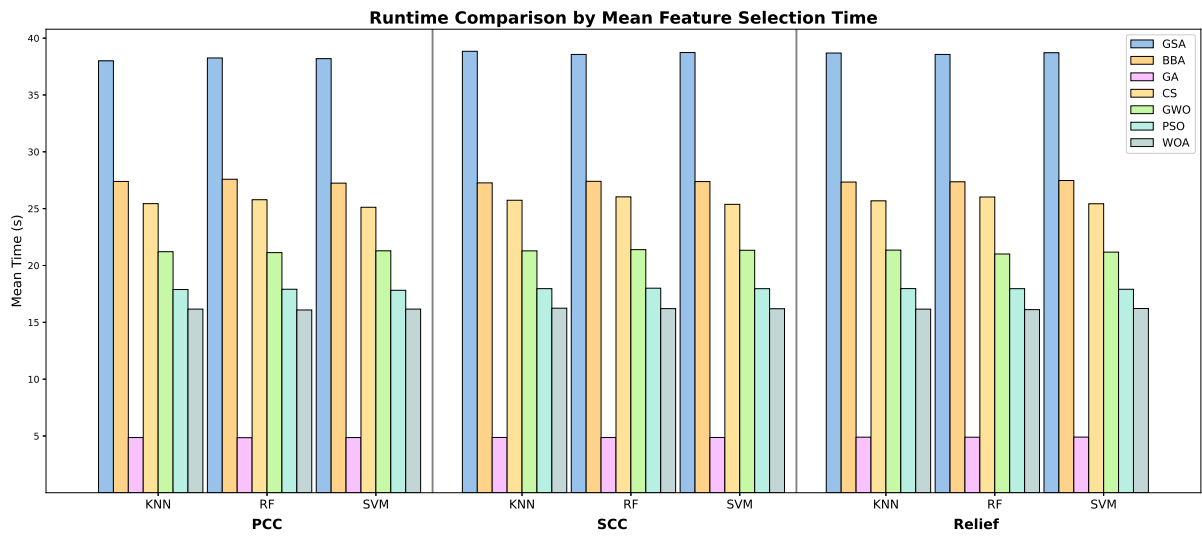
Table 5: Comparative Performance Analysis with State-Of-The-Art

Model	Accuracy	Std. Dev.	Train Time (s)
LandNet [9]	0.974	0.0140	80.72
AngleNet [9]	0.975	0.0130	53.32
ConcatNet [9]	0.986	0.0120	47.45
Random Forest + PCA [10]	0.950	0.1136	–
ViT-B (Transformer) [6]	0.948	0.8300	–
ConvNeXt-Base (CNN) [6]	0.950	0.0100	–
Swin-V2-B (Transformer) [6]	0.932	0.0083	–
ShuffleNetV2-X2 (CNN) [6]	0.954	0.0114	–
ResNet-152 (CNN) [6]	0.940	<b>0.0071</b>	–
MaxViT-T (CNN + Transformer) [6]	0.954	0.0182	–
<b>Relief + GSA + RF (ours)</b>	<b>0.991</b>	0.0100	<b>39.10</b>

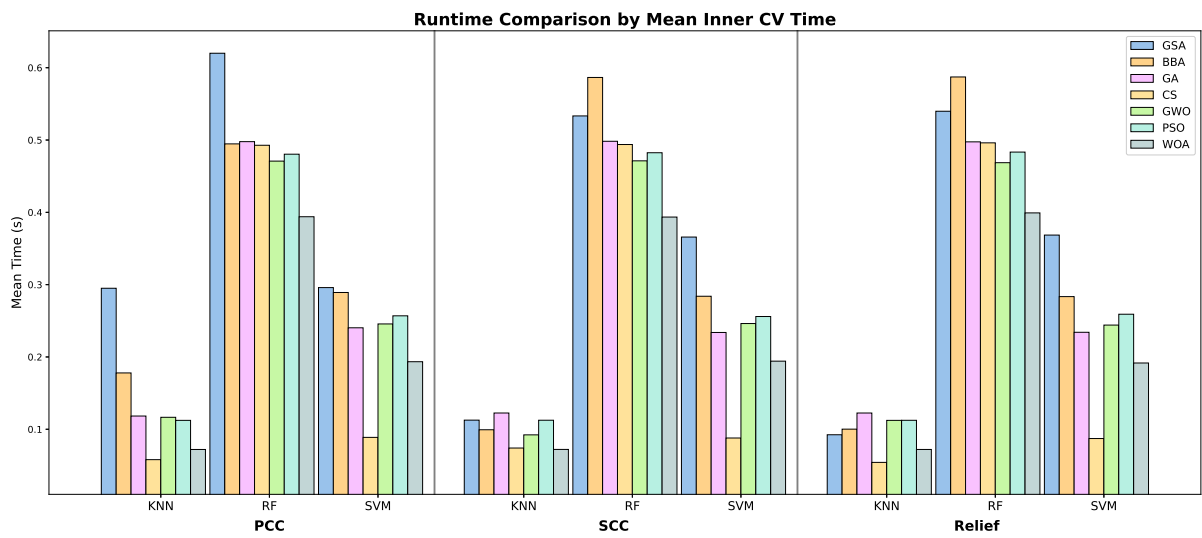
PCA [10], yielded notably lower accuracy (0.950) and exhibited instability as reflected by a larger standard deviation (0.1136). Similarly, skeleton-based dual-stream deep learning methods [6], encompassing both convolutional and transformer backbones, exhibited performance clustered within the 0.932 – 0.954 range. However, their robustness varied distinctly, with models such as ViT-B yielding highly unstable outputs (standard deviation 0.8300), raising concerns about their generalizability. An additional distinguishing factor of the proposed method lies in its computational efficiency. Specifically, Relief + GSA + RF achieved the lowest recorded training time (39.10 sec), substantially outperforming the training times of the neural architectures from [9], which ranged from 47.45 sec to 80.72 sec. Collectively, these findings underscore that the integration of targeted feature reduction strategies with ensemble learning provides a compelling alternative to purely deep learning-based solutions, offering an improved balance between accuracy, robustness, and computational practicality.

## 6 Conclusion and discussions

The increasing global prevalence of ASD underscores the urgent need for reliable, efficient, and accurate methods for its early prediction and intervention. This study addresses this pressing problem using a 3D walking video dataset by integrating correlation-based ranking coefficients, nature-inspired optimization algorithms for feature selection, and supervised machine learning classifiers. Unlike prior approaches,



(a) Runtime comparison of mean feature selection time



(b) Runtime comparison of mean inner cross-validation time

Fig. 8: Runtime comparisons of various combinations of feature extraction and classification algorithms

the proposed methodology demonstrates a superior balance between accuracy, feature reduction, and computational efficiency, establishing new performance benchmarks in ASD detection.

Among all evaluated combinations, two distinct configurations emerged as particularly effective. The setup involving the Relief ranking coefficient, CS for feature selection, and RF as the classifier achieved an accuracy of 96.875% with only 4 features, corresponding to a remarkable reduction of 99.68%. This makes it highly suitable for scenarios prioritizing model compactness and resource efficiency. On the other hand, the integration of the Relief coefficient, GSA, and RF achieved perfect accuracy (100%) with a 69.81% feature reduction, thereby setting a new performance ceiling for ASD detection with state-of-the-art efficiency (training time  $\approx$  39s). Furthermore, comparative analysis with existing deep learning-based methods confirms that the proposed Relief+GSA+RF framework not only surpasses them in terms of accuracy but also provides greater robustness with significantly lower computational burden. The experimental findings highlight the potential of combining correlation-driven initialization, feature selection via nature-inspired algorithms, and classification strategies to address complex neurodevelopmental diagnostic tasks. Future extensions of this work should include large-scale datasets with greater variability to validate generalizability and to further enhance adaptability and real-world deployment. In particular, modifications to the GSA for alternative distance functions and multi-dimensional optimization may expand its applicability in broader feature extraction tasks.

Overall, the proposed methodology demonstrates that robust feature selection, when coupled with an efficient classification pipeline, can significantly improve both prediction accuracy and computational feasibility for ASD detection from video data. With perfect diagnostic accuracy achieved in the best configuration, the model shows practical potential for integration into healthcare workflows, thereby contributing to early identification and improved treatment planning for individuals with ASD. Continuous research and refinement remain essential to ensure scalability across diverse populations and to enable real-time deployment through computer vision-based systems in clinical practice.

## Declarations

### Ethical Approval

This study involved secondary analysis of a publicly available dataset and did not require additional ethical approval.

### Consent to Participate

Not applicable.

### Consent to Publish

Not applicable.

### Data Availability Statement

We used the publicly available dataset [7], "Three-Dimensional Dataset Combining Gait and Full Body Movement of Children with Autism Spectrum Disorders Collected by Kinect v2 Camera Dataset," which can be accessed from <https://datadryad.org/dataset/doi:10.5061/dryad.s7h44j150>.

### Authors Contributions

**Aneesh Panchal:** Writing - original draft, Methodology, Investigation, Conceptualization. **Kainat Khan:** Writing - original draft, Supervision. **Rahul Katarya:** Writing - review & editing, Supervision.

### Funding

This research received no specific grant from any funding agency in the public, commercial, or not-for-profit sectors.

### Competing Interests

The authors declare that they have no known competing interests.

## References

- [1] Mahmoud Elbattah, Jean-Luc Guérin, Romuald Carette, Federica Cilia, and Gilles Dequen. Nlp-based approach to detect autism spectrum disorder in saccadic eye movement. In *2020 IEEE Symposium Series on Computational Intelligence (SSCI)*, pages 1581–1587. IEEE, 2020.
- [2] Zhi Zheng, Qiang Fu, Huan Zhao, Amy R Swanson, Amy S Weitlauf, Zachary E Warren, and Nilanjan Sarkar. Design of an autonomous social orienting training system (asots) for young children with autism. *IEEE Transactions on Neural Systems and Rehabilitation Engineering*, 25(6):668–678, 2016.
- [3] Akshay Puli and Azadeh Kushki. Toward automatic anxiety detection in autism: A real-time algorithm for detecting physiological arousal in the presence of motion. *IEEE Transactions on Biomedical Engineering*, 67(3):646–657, 2019.
- [4] Jing Li, Yihao Zhong, Junxia Han, Gaoxiang Ouyang, Xiaoli Li, and Honghai Liu. Classifying asd children with lstm based on raw videos. *Neurocomputing*, 390:226–238, 2020.
- [5] Jung Hyuk Lee, Geon Woo Lee, Guiyoung Bong, Hee Jeong Yoo, and Hong Kook Kim. Deep-learning-based detection of infants with autism spectrum disorder using auto-encoder feature representation. *Sensors*, 20(23):6762, 2020.
- [6] Jungpil Shin, Abu Saleh Musa Miah, Manato Kakizaki, Najmul Hassan, and Yoichi Tomioka. Autism spectrum disorder detection using skeleton-based body movement analysis via dual-stream deep learning. *Electronics*, 14(11):2231, 2025.
- [7] Ahmed A Al-Jubouri, Israa Hadi Ali, and Yasen Rajihy. Generating 3d dataset of gait and full body movement of children with autism spectrum disorders collected by kinect v2 camera. *CompuSoft*, 9(8):3791–3797, 2020.
- [8] Mina Zeraati and Amirehsan Davoodi. Asd-graphnet: A novel graph learning approach for autism spectrum disorder diagnosis using fmri data. *Computers in Biology and Medicine*, 196:110723, 2025.
- [9] Federica Colonnese, Francesco Di Luzio, Antonello Rosato, and Massimo Panella. Bimodal feature analysis with deep learning for autism spectrum disorder detection. *International Journal of Neural Systems*, 34(02):2450005, 2024.
- [10] Sumaiya Abul Kalam, Tasnia Rahman Prome, and Muhammad Ahsan Ullah. Machine learning approach for identification of autism spectrum disorder from video using openpose. In *2024 27th International Conference on Computer and Information Technology (ICCIT)*, pages 1720–1725. IEEE, 2024.
- [11] Benn Henderson, Yogarajah Pratheepan, Bryan Gardiner, and T Martin McGinnity. 3d human pose estimation model analysis: Gait analytics for autism spectrum disorder detection. In *2023 31st Irish Conference on Artificial Intelligence and Cognitive Science (AICS)*, pages 1–4. IEEE, 2023.
- [12] S Malathi and D Kannan. Adaptive whale optimization based support vector machine for prediction of autism spectrum disorder. *Journal of Theoretical and Applied Information Technology*, 100(9), 2022.
- [13] Sanat Kumar Sahu and Pratibha Verma. Classification of autistic spectrum disorder using deep neural network with particle swarm optimization. *International Journal of Computer Vision and Image Processing (IJCVIP)*, 12(1):1–11, 2022.
- [14] S Malathi and D Kannan. Robust artificial bee colony optimization based classifier for prediction of autism spectrum disorder. In *2022 International Conference on Advanced Computing Technologies and Applications (ICACTA)*, pages 1–5. IEEE, 2022.
- [15] A Saranya and Rangasamy Anandan. Autism spectrum prognosis using worm optimized extreme learning machine (woem) technique. In *2021 international conference on advance computing and innovative technologies in engineering (icacite)*, pages 636–641. IEEE, 2021.
- [16] Basma Elshoky, Osman Ali Sadek Ibrahim, and Abdelmgeid Amin Ali. Machine learning techniques based on feature selection for improving autism disease classification. *International Journal of Intelligent Computing and Information Sciences*, 21(2):65–81, 2021.

- [17] K Balakrishnan et al. Detecting autism spectrum disorder with sailfish optimisation. *Indian Journal of Radio & Space Physics (IJRSP)*, 50(2):68–73, 2022.
- [18] Nikita Goel, Bhavya Grover, Deepak Gupta, Ashish Khanna, Moolchand Sharma, et al. Modified grasshopper optimization algorithm for detection of autism spectrum disorder. *Physical Communication*, 41:101115, 2020.
- [19] Mochammad Farrell, Kurniawan Nur Ramadhani, and Suyanto Suyanto. Combined firefly algorithm-random forest to classify autistic spectrum disorders. In *2020 3rd international seminar on research of information technology and intelligent systems (ISRITI)*, pages 505–508. IEEE, 2020.
- [20] R Abitha and S Mary Vennila. A swarm based symmetrical uncertainty feature selection method for autism spectrum disorders. In *2019 Third International Conference on Inventive Systems and Control (ICISC)*, pages 665–669. IEEE, 2019.
- [21] Manar D Samad, Norou Diawara, Jonna L Bobzien, John W Harrington, Megan A Witherow, and Khan M Iftekharuddin. A feasibility study of autism behavioral markers in spontaneous facial, visual, and hand movement response data. *IEEE Transactions on Neural Systems and Rehabilitation Engineering*, 26(2):353–361, 2017.
- [22] Patrick Schober, Christa Boer, and Lothar A Schwarte. Correlation coefficients: appropriate use and interpretation. *Anesthesia & analgesia*, 126(5):1763–1768, 2018.
- [23] Mavuto M Mukaka. A guide to appropriate use of correlation coefficient in medical research. *Malawi medical journal*, 24(3):69–71, 2012.
- [24] R Porkodi. Comparison of filter based feature selection algorithms: an overview. *International journal of Innovative Research in Technology & Science*, 2(2):108–113, 2014.
- [25] Ashraf Darwish. Bio-inspired computing: Algorithms review, deep analysis, and the scope of applications. *Future Computing and Informatics Journal*, 3(2):231–246, 2018.
- [26] S Binitha, S Siva Sathya, et al. A survey of bio inspired optimization algorithms. *International journal of soft computing and engineering*, 2(2):137–151, 2012.
- [27] Xin-She Yang and Xingshi He. Nature-inspired optimization algorithms in engineering: overview and applications. *Nature-inspired computation in engineering*, pages 1–20, 2016.
- [28] Himanshu Mittal, Ashish Tripathi, Avinash Chandra Pandey, and Raju Pal. Gravitational search algorithm: a comprehensive analysis of recent variants. *Multimedia Tools and Applications*, 80(5):7581–7608, 2021.
- [29] Xiao-Xu Ma and Jie-Sheng Wang. Optimized parameter settings of binary bat algorithm for solving function optimization problems. *Journal of Electrical and Computer Engineering*, 2018(1):3847951, 2018.
- [30] Xin-She Yang and Suash Deb. Cuckoo search via lévy flights. In *2009 World congress on nature & biologically inspired computing (NaBIC)*, pages 210–214. Ieee, 2009.
- [31] Yuxiang Hou, Huanbing Gao, Zijian Wang, and Chuansheng Du. Improved grey wolf optimization algorithm and application. *Sensors*, 22(10):3810, 2022.
- [32] Gui-Ying Ning and Dun-Qian Cao. Improved whale optimization algorithm for solving constrained optimization problems. *Discrete Dynamics in Nature and Society*, 2021(1):8832251, 2021.
- [33] Suman Raj and Sarfaraz Masood. Analysis and detection of autism spectrum disorder using machine learning techniques. *Procedia Computer Science*, 167:994–1004, 2020.
- [34] Folorunso Y Osisanwo, Joseph ET Akinsola, Oludele Awodele, John O Himmikaiye, Oluwole Olakanmi, Joseph Akinjobi, et al. Supervised machine learning algorithms: classification and comparison. *International Journal of Computer Trends and Technology (IJCTT)*, 48(3):128–138, 2017.
- [35] Ritam Guha, Bitanu Chatterjee, SK Khalid Hassan, Shameem Ahmed, Trinav Bhattacharyya, and Ram Sarkar. Py\_fs: a python package for feature selection using meta-heuristic optimization algorithms. In *Computational Intelligence in Pattern Recognition: Proceedings of CIPR 2021*, pages 495–504. Springer, 2021.

# Appendix

## Extended Results and Explanations

Table 6 summarizes the single-case test accuracy, precision, recall, and F1-score for various combinations of nature-inspired optimization algorithms (optimizers), classifiers, and feature ranking coefficients. Overall, the results indicate that SVM consistently performs the worst among the classifiers evaluated.

Table 6: Test Accuracy (Acc.), Precision (Prec.), Recall (Rec.), and F1-Score (F1) (%)

Ranking	Optimizer	KNN				RF				SVM			
		Acc.	Prec.	Rec.	F1	Acc.	Prec.	Rec.	F1	Acc.	Prec.	Rec.	F1
PCC	GSA	98.75	98.75	98.75	98.75	95.62	95.69	95.62	95.62	80.62	86.04	80.62	79.87
	BBA	96.88	96.94	96.88	96.87	96.25	96.28	96.25	96.25	66.88	66.90	66.88	66.86
	GA	98.75	98.78	98.75	98.75	<b>97.50</b>	<b>97.50</b>	<b>97.50</b>	<b>97.50</b>	<b>85.00</b>	<b>87.86</b>	<b>85.00</b>	<b>84.71</b>
	CS	<b>99.38</b>	<b>99.38</b>	<b>99.38</b>	<b>99.37</b>	96.25	96.28	96.25	96.25	80.62	81.46	80.62	80.50
	GWO	98.12	98.19	98.12	98.12	97.50	97.53	97.50	97.50	65.62	66.56	65.62	65.13
	PSO	98.75	98.78	98.75	98.75	96.25	96.28	96.25	96.25	71.25	78.33	71.25	69.33
	WOA	98.75	98.75	98.75	98.75	96.25	96.28	96.25	96.25	81.88	85.97	81.88	81.34
SCC	GSA	98.12	98.13	98.12	98.12	96.88	96.88	96.88	96.87	66.88	78.43	66.88	63.13
	BBA	98.12	98.19	98.12	98.12	97.50	97.62	97.50	97.50	69.38	69.62	69.38	69.28
	GA	<b>98.75</b>	<b>98.78</b>	<b>98.75</b>	<b>98.75</b>	97.50	97.50	97.50	97.50	<b>85.00</b>	<b>87.86</b>	<b>85.00</b>	<b>84.71</b>
	CS	93.12	93.46	93.12	93.11	95.62	95.69	95.62	95.62	78.75	83.45	78.75	77.98
	GWO	96.88	97.06	96.88	96.87	<b>98.12</b>	<b>98.19</b>	<b>98.12</b>	<b>98.12</b>	75.62	80.88	75.62	74.54
	PSO	98.12	98.19	98.12	98.12	95.62	95.69	95.62	95.62	77.50	82.74	77.50	76.56
	WOA	98.12	98.13	98.12	98.12	96.25	96.28	96.25	96.25	71.25	79.34	71.25	69.12
Relief	GSA	97.50	97.50	97.50	97.50	<b>98.75</b>	<b>98.78</b>	<b>98.75</b>	<b>98.75</b>	70.00	78.67	70.00	67.55
	BBA	97.50	97.53	97.50	97.50	<b>98.75</b>	<b>98.78</b>	<b>98.75</b>	<b>98.75</b>	63.75	64.32	63.75	63.38
	GA	98.75	98.78	98.75	98.75	97.50	97.50	97.50	97.50	<b>85.00</b>	<b>87.86</b>	<b>85.00</b>	<b>84.71</b>
	CS	<b>99.38</b>	<b>99.38</b>	<b>99.38</b>	<b>99.37</b>	96.25	96.28	96.25	96.25	80.62	81.46	80.62	80.50
	GWO	98.12	98.19	98.12	98.12	97.50	97.53	97.50	97.50	65.62	66.56	65.62	65.13
	PSO	98.75	98.78	98.75	98.75	96.25	96.28	96.25	96.25	71.25	78.33	71.25	69.33
	WOA	98.75	98.75	98.75	98.75	96.25	96.28	96.25	96.25	81.88	85.97	81.88	81.34

Table 7 reports the nested cross-validation outcomes, including mean accuracy, standard deviation, and 95% confidence intervals for the different algorithmic combinations. Consistent with the previous findings, SVM exhibits the poorest performance, characterized by low accuracy and high variability.

Table 7: Nested Cross-Validation Results: Mean Accuracy (Acc.), Standard Deviation (SD), and Confidence Intervals (CI)

Ranking	Optimizer	KNN			RF			SVM		
		Acc.	SD	CI	Acc.	SD	CI	Acc.	SD	CI
PCC	GSA	97.37	0.02	[95.19, 98.75]	97.88	0.02	[95.75, 99.31]	74.50	0.14	[69.75, 80.19]
	BBA	96.00	0.02	[93.38, 97.44]	97.88	0.03	[96.25, 100.00]	70.50	0.32	[61.81, 76.19]
	GA	<b>98.00</b>	<b>0.02</b>	<b>[95.81, 99.31]</b>	98.50	0.02	[96.94, 100.00]	<b>75.62</b>	<b>0.27</b>	<b>[70.25, 84.19]</b>
	CS	95.88	0.04	[94.38, 99.06]	97.38	0.03	[95.12, 99.38]	71.38	0.85	[58.44, 82.31]
	GWO	97.12	0.00	[96.31, 98.06]	<b>98.62</b>	<b>0.02</b>	<b>[96.94, 100.00]</b>	69.75	0.23	[62.81, 74.31]
	PSO	98.00	0.00	[97.50, 98.75]	98.00	0.02	[96.31, 99.94]	72.50	0.04	[70.69, 75.44]
	WOA	97.50	0.01	[96.25, 98.75]	97.50	0.02	[96.25, 99.31]	74.63	0.16	[70.69, 81.25]
SCC	GSA	97.50	0.00	[96.88, 98.12]	97.88	0.02	[96.31, 99.94]	70.62	0.09	[67.12, 75.25]
	BBA	95.62	0.04	[92.75, 98.00]	98.38	0.01	[97.50, 99.38]	70.50	0.14	[66.38, 75.94]
	GA	<b>98.00</b>	<b>0.02</b>	<b>[95.81, 99.31]</b>	98.50	0.02	[96.94, 100.00]	<b>75.62</b>	<b>0.27</b>	<b>[70.25, 84.19]</b>
	CS	96.63	0.04	[93.44, 98.69]	97.75	0.02	[95.75, 99.88]	68.75	0.42	[62.50, 78.25]
	GWO	96.50	0.04	[93.44, 98.62]	<b>98.75</b>	<b>0.01</b>	<b>[97.56, 99.94]</b>	72.88	0.04	[70.12, 75.50]
	PSO	97.88	0.02	[95.31, 99.31]	97.88	0.03	[95.75, 99.94]	75.00	0.12	[70.31, 79.75]
	WOA	97.38	0.04	[94.06, 99.81]	98.38	0.02	[96.38, 99.94]	69.00	0.14	[64.62, 74.62]
Relief	GSA	<b>98.37</b>	<b>0.01</b>	<b>[97.50, 99.88]</b>	<b>99.12</b>	<b>0.01</b>	<b>[97.62, 100.00]</b>	71.00	0.17	[65.38, 76.12]
	BBA	96.25	0.08	[92.12, 99.25]	98.75	0.01	[97.06, 99.94]	68.88	0.18	[63.75, 73.56]
	GA	98.00	0.02	[95.81, 99.31]	98.50	0.02	[96.94, 100.00]	<b>75.62</b>	<b>0.27</b>	<b>[70.25, 84.19]</b>
	CS	95.88	0.04	[94.38, 99.06]	97.38	0.03	[95.12, 99.38]	71.38	0.85	[58.44, 82.31]
	GWO	97.12	0.00	[96.31, 98.06]	98.62	0.02	[96.94, 100.00]	69.75	0.23	[62.81, 74.31]
	PSO	98.00	0.00	[97.50, 98.75]	98.00	0.02	[96.31, 99.94]	72.50	0.04	[70.69, 75.44]
	WOA	97.50	0.01	[96.25, 98.75]	97.50	0.02	[96.25, 99.31]	74.63	0.16	[70.69, 81.25]

Table 8 presents the results of outer cross-validation across multiple folds using the same combinations, further demonstrating the superior performance of KNN and RF classifiers over the SVM approach.

Table 8: Outer Cross-Validation Accuracy (%) over Folds {F1, F2, F3, F4, F5}

Ranking	Optimizer	KNN					RF					SVM				
		F1	F2	F3	F4	F5	F1	F2	F3	F4	F5	F1	F2	F3	F4	F5
PCC	GSA	95.00	96.88	97.50	98.75	98.75	98.75	99.38	98.75	96.88	95.62	73.12	69.38	76.25	73.12	80.62
	BBA	97.50	93.12	95.62	96.88	96.88	100.00	96.25	100.00	96.88	96.25	75.62	61.25	72.50	76.25	66.88
	GA	98.75	97.50	95.62	99.38	98.75	100.00	98.12	100.00	96.88	97.50	72.50	70.00	73.75	76.88	85.00
	CS	95.00	94.38	96.25	94.38	99.38	99.38	95.00	99.38	96.88	96.25	66.88	69.38	82.50	57.50	80.62
	GWO	96.88	96.88	96.25	97.50	98.12	100.00	98.75	100.00	96.88	97.50	62.50	73.75	74.38	72.50	65.62
	PSO	97.50	97.50	97.50	98.75	98.75	100.00	97.50	99.38	96.88	96.25	75.62	73.75	71.25	70.62	71.25
	WOA	97.50	96.25	96.25	98.75	98.75	98.75	96.25	99.38	96.88	96.25	70.62	71.25	73.75	75.62	81.88
SCC	GSA	96.88	97.50	98.12	96.88	98.12	99.38	96.25	100.00	96.88	96.88	69.38	69.38	75.62	71.88	66.88
	BBA	96.88	92.50	95.00	95.62	98.12	99.38	98.12	99.38	97.50	97.50	76.25	66.25	67.50	73.12	69.38
	GA	98.75	97.50	95.62	99.38	98.75	100.00	98.12	100.00	96.88	97.50	72.50	70.00	73.75	76.88	85.00
	CS	96.88	96.25	98.75	98.12	93.12	100.00	96.88	98.75	97.50	95.62	62.50	62.50	73.75	66.25	78.75
	GWO	97.50	98.75	93.12	96.25	96.88	99.38	98.75	100.00	97.50	98.12	73.12	70.00	71.25	74.38	75.62
	PSO	98.12	99.38	95.00	98.75	98.12	100.00	97.50	99.38	96.88	95.62	80.00	70.00	74.38	73.12	77.50
	WOA	100.00	93.75	98.12	96.88	98.12	100.00	98.75	99.38	97.50	96.25	64.38	66.88	75.00	67.50	71.25
Relief	GSA	100.00	97.50	98.12	98.75	97.50	100.00	99.38	100.00	97.50	98.75	75.00	65.00	76.25	68.75	70.00
	BBA	98.12	99.38	91.88	94.38	97.50	100.00	98.75	99.38	96.88	98.75	71.25	71.88	73.75	63.75	63.75
	GA	98.75	97.50	95.62	99.38	98.75	100.00	98.12	100.00	96.88	97.50	72.50	70.00	73.75	76.88	85.00
	CS	95.00	94.38	96.25	94.38	99.38	99.38	95.00	99.38	96.88	96.25	66.88	69.38	82.50	57.50	80.62
	GWO	96.88	96.88	96.25	97.50	98.12	100.00	98.75	100.00	96.88	97.50	62.50	73.75	74.38	72.50	65.62
	PSO	97.50	97.50	97.50	98.75	98.75	100.00	97.50	99.38	96.88	96.25	75.62	73.75	71.25	70.62	71.25
	WOA	97.50	96.25	96.25	98.75	98.75	98.75	96.25	99.38	96.88	96.25	70.62	71.25	73.75	75.62	81.88

Table 9 details the average feature selection time, cross-validation time, and the average number of features selected for each combination. These results highlight the efficiency of the GA in computational time and the effectiveness of the CS algorithm in minimizing the number of selected features.

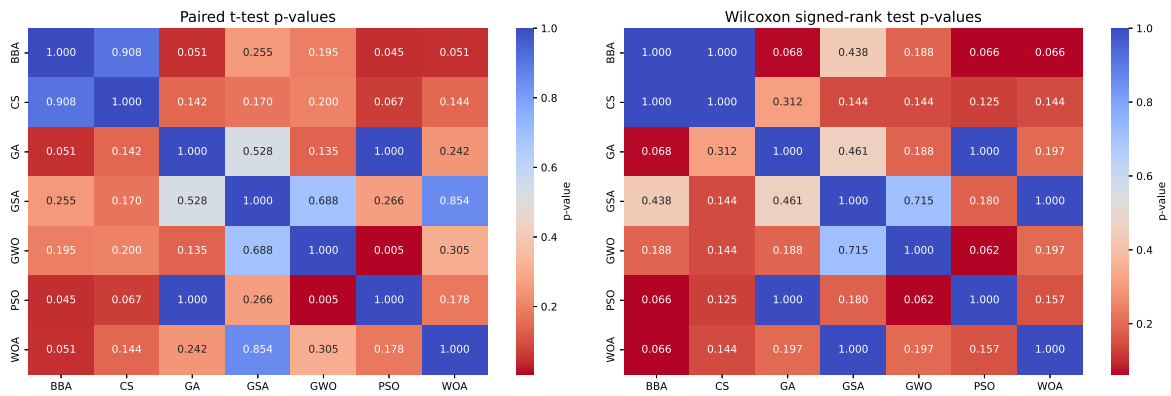
Table 9: Feature Selection (FS) time (in sec), Cross Validation (CV) time (in sec), and Mean number of features selected (#Feat.)

Ranking	Optimizer	KNN			RF			SVM		
		FS Time	CV Time	#Feat.	FS Time	CV Time	#Feat.	FS Time	CV Time	#Feat.
PCC	GSA	38.00	0.295	409.6	38.26	0.620	405.8	38.19	0.296	431.4
	BBA	27.39	0.178	302.8	27.59	0.495	324.0	27.24	0.289	283.8
	GA	<b>4.86</b>	0.118	298.6	<b>4.85</b>	0.498	298.6	<b>4.86</b>	0.240	298.6
	CS	25.44	<b>0.058</b>	<b>160.0</b>	25.79	0.493	326.0	25.12	<b>0.089</b>	<b>94.4</b>
	GWO	21.21	0.117	352.0	21.13	<b>0.471</b>	318.6	21.29	0.246	304.8
	PSO	17.89	0.112	351.0	17.91	0.480	328.4	17.82	0.257	344.8
	WOA	16.16	0.072	215.4	16.09	0.394	<b>226.2</b>	16.16	0.193	232.6
SCC	GSA	38.84	0.113	407.8	38.56	0.533	404.4	38.73	0.366	410.6
	BBA	27.27	0.099	338.0	27.40	0.587	319.2	27.38	0.284	302.6
	GA	<b>4.87</b>	0.122	298.6	<b>4.87</b>	0.498	298.6	<b>4.87</b>	0.234	298.6
	CS	25.74	0.074	320.2	26.04	0.494	297.6	25.38	<b>0.088</b>	307.0
	GWO	21.29	0.092	317.6	21.39	<b>0.471</b>	304.0	21.34	0.246	304.4
	PSO	17.96	0.112	329.4	18.00	0.482	339.8	17.96	0.256	340.6
	WOA	16.24	<b>0.072</b>	<b>223.0</b>	16.21	0.393	<b>195.8</b>	16.19	0.194	<b>237.4</b>
Relief	GSA	38.69	0.092	394.2	38.56	0.540	406.8	38.71	0.369	413.2
	BBA	27.34	0.100	278.4	27.36	0.587	299.0	27.47	0.283	310.2
	GA	<b>4.90</b>	0.122	298.6	<b>4.89</b>	0.497	298.6	<b>4.90</b>	0.234	298.6
	CS	25.69	<b>0.054</b>	<b>160.0</b>	26.03	0.496	<b>34.5</b>	25.43	<b>0.087</b>	<b>94.4</b>
	GWO	21.35	0.112	352.0	21.01	0.469	318.6	21.18	0.244	304.8
	PSO	17.97	0.112	351.0	17.96	0.483	328.4	17.91	0.259	344.8
	WOA	16.16	0.072	215.4	16.12	<b>0.399</b>	226.2	16.22	0.192	232.6

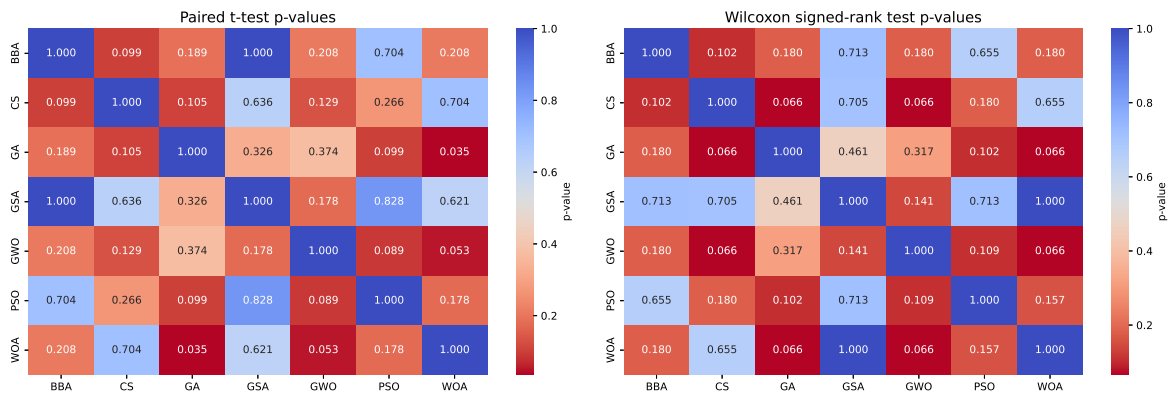
## Statistical Test Results

From Figs. 9, 10, and 11, it can be inferred that most nature-inspired feature selection algorithms yield statistically similar classification performances when combined with KNN and SVM classifiers. However, certain pairings, particularly those involving the RF classifier, exhibit significant or borderline differences. Additionally, variations among the different feature selection algorithms are apparent. Across all cases, it is evident that the Relief ranking coefficients combined with the RF classifier consistently achieve the best performance.

### PCC - KNN Statistical Test p-values



### PCC - RF Statistical Test p-values



### PCC - SVM Statistical Test p-values

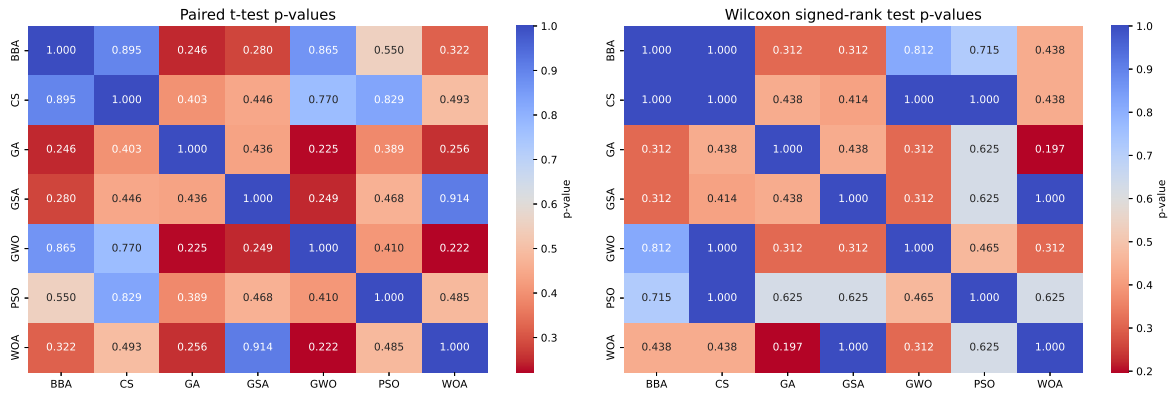
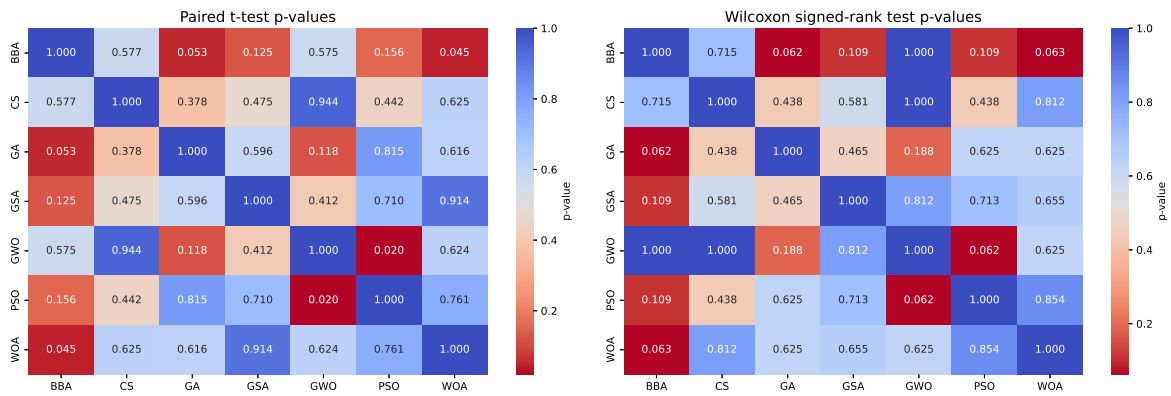
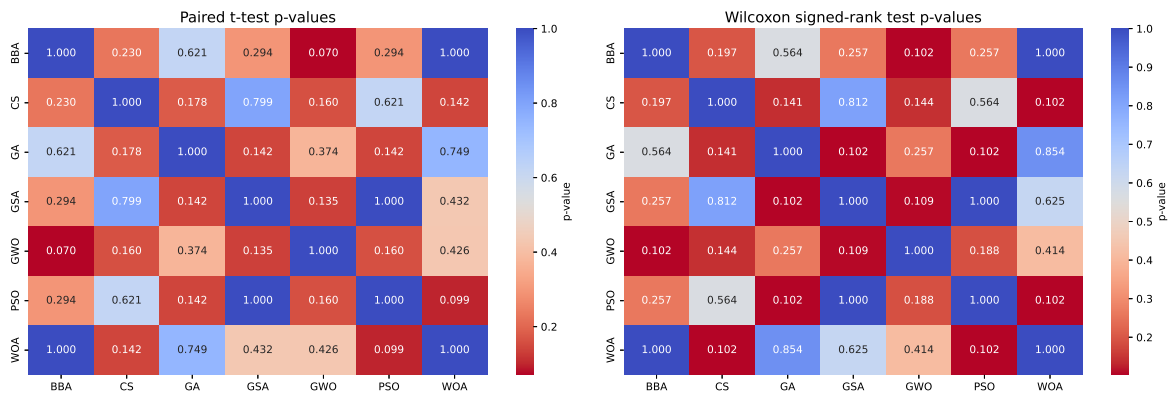


Fig. 9: Statistical tests for PCC

### SCC - KNN Statistical Test p-values



### SCC - RF Statistical Test p-values



### SCC - SVM Statistical Test p-values

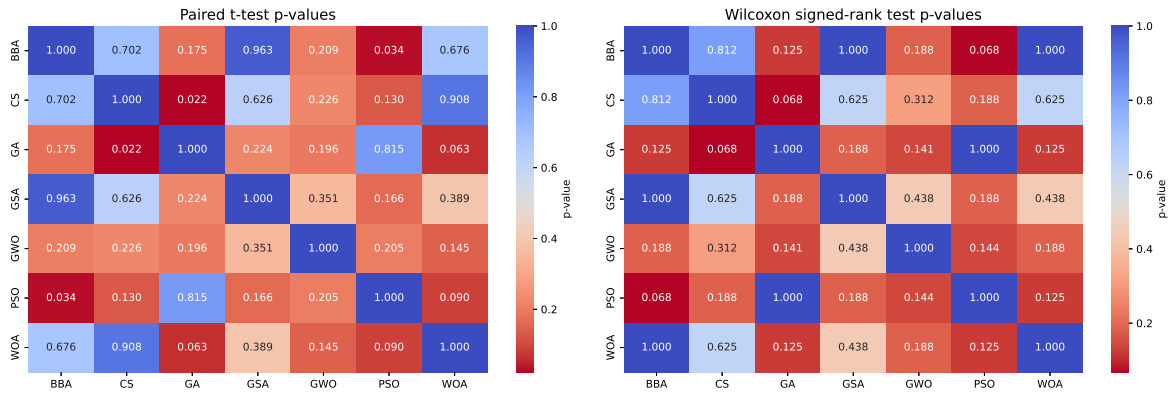
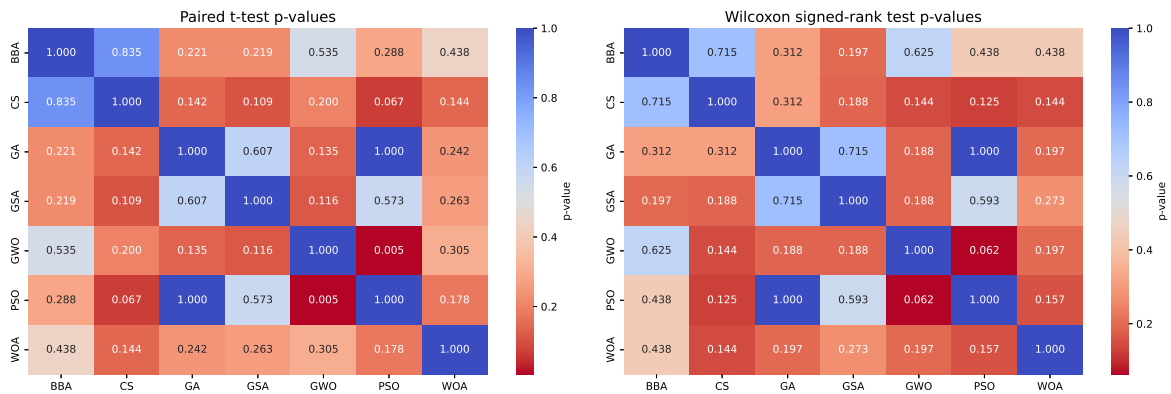
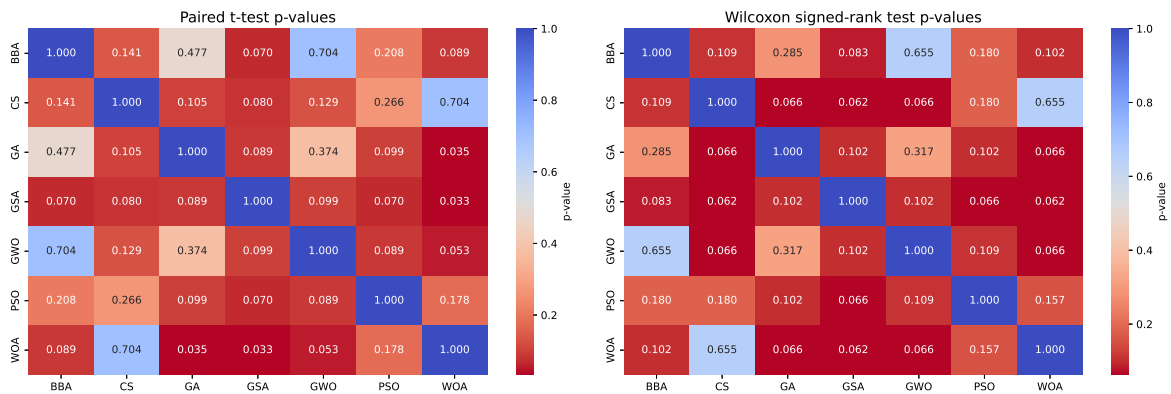


Fig. 10: Statistical tests for SCC

### Relief - KNN Statistical Test p-values



### Relief - RF Statistical Test p-values



### Relief - SVM Statistical Test p-values

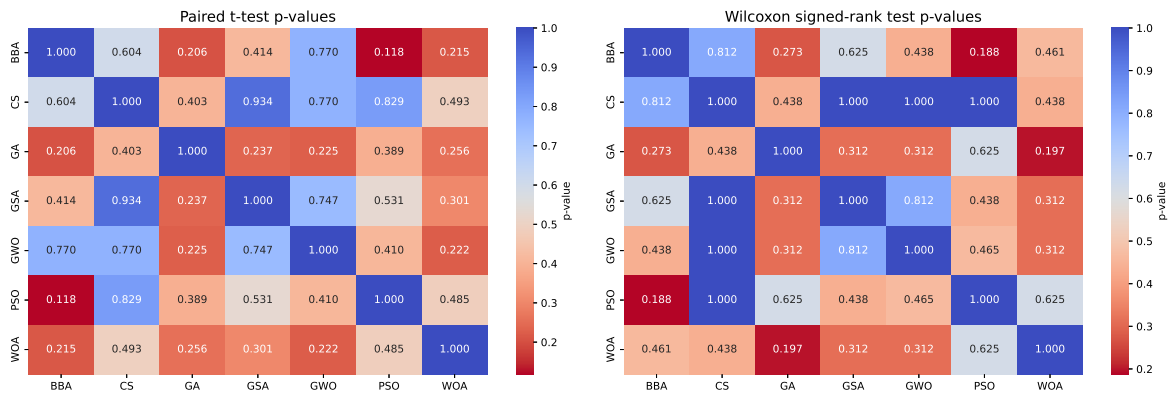


Fig. 11: Statistical tests for Relief ranking coefficient